Geological Quarterly, 2022, 66: 33
DOI: http://dx.doi.org/10.7306/gq.1665

High-energy, microtidal nearshore deposits and their provenance (Lower Miocene, Burdigalian/Eggenburgian, Alpine-Carpathian Foredeep, Lower Austria)

Slavomír NEHYBA [1, *] and Reinhard ROETZEL [2]

[1] Masaryk University, Department of Geological Sciences, Faculty of Science, Kotlářská 2, CZ- 611 37 Brno, Czech Republic; ORCID: 0000-0001-5778-0819

[2] Geological Survey, Neulinggasse 38, A-1030 Wien, Austria

Nehyba, S., Roetzel, R., 2022. High-energy, microtidal nearshore deposits and their provenance (Lower Miocene, Burdigalian/Eggenburgian, Alpine-Carpathian Foredeep, Lower Austria). Geological Quarterly, 66: 33, doi: 10.7306/gq.1665

During the Early Miocene (Early Burdigalian/Eggenburgian) marine transgression at the southeastern margin of the Bohemian Massif, gradual flooding occurred along a rocky coast on granitic bedrock of the Thaya Batholith under high-energy, wave-dominated, microtidal and mixed fair-weather and storm conditions. Deposits of the Burgschleinitz Formation overlie a basal unconformity above a subaerial weathered basement surface (transgressive erosional surface) and are interpreted as a transgressive systems tract. The deposits can be divided into four facies associations/depositional environments, i.e., upper-shoreface, foreshore, gravelly beach and backshore/lagoon. Two stages of transgression and successive overtopping of the basement, with different coastal physiographies, were documented. During the initial stage of transgression a barrier island system developed with relatively fine-grained deposits, reflecting the flooding of the distant parts of the Thaya Batholith with a relative flat basement morphology. The subsequent continuation of the transgression led to the flooding of the more proximal parts of the Thaya Batholith with a steeper relief and formation of a rocky shoreline with deposition of gravelly sediments along palaeo-sea cliffs or wave-cut platforms. While gravel clasts of the deposits investigated originate directly from the underlying granites of the Thaya Batholith, provenance studies show that metamorphic rocks of the Moravian Superunit in the hinterland were the main source of sands. This distant source material was probably delivered mainly by small creeks and alluvial fans to the nearshore. Significant differences in heavy mineral composition of the same formation in the wider vicinity indicate primarily local sources and rapid deposition with subordinate longshore transport, which may reflect a complex coastal palaeogeography. The Lower Miocene deposits of the Burgschleinitz Formation investigated are a rare example of ancient rocky shore deposits, which generally have low preservation potential in the geological record.

Key words: Alpine-Carpathian Foredeep, Lower Miocene, provenance analysis, fair-weather vs. storm processes, rocky shoreline, coastal morphology.

INTRODUCTION

The dynamics of shallow marine processes and coastal physiography are the principal parameters recorded in the distinctive stratigraphic architecture of coastal facies (Cattaneo and Steel, 2003; Yoshida et al., 2007; Zecchin, 2007; Longhitano et al., 2012; Nalin et al., 2016). Conditions suitable for identification of such parameters and solving stratigraphic questions in the fossil sedimentary record typically include extensive exposures commonly with 3D accessibility, extraordinary preservation and availability of primary sedimentary structures, known relationships to the palaeo-coastline, and excellent chronostratigraphic control (Nalin and Massari, 2018). These conditions are difficult to meet in most sedimentary basins of Central Europe, where the detection of depositional processes and stratigraphy are mostly limited to small, isolated exposures and/or subsurface data. Therefore, the recognition of sedimentary conditions that reflect a complex set of processes affecting coastal settings (ambient energy, wave climate, tidal range, biogenic processes, palaeogeographic configuration, sediment supply, grain size of available material, base level changes…) may be challenging in such a situation.

We provide a sedimentological analysis of nearshore deposits of the Lower Miocene (Eggenburgian) Burgschleinitz Formation in the Alpine-Carpathian Foredeep, where sand and gravel pits provide exposures revealing abundant sedimentary structures suitable for identification of the depositional environment and measurement of palaeocurrent directions, and where the approximate palaeo-coastline configuration can be reliably reconstructed from detailed geological mapping and provenance analysis. The goals of this study are: (1) to identify the depositional environment and the coastal processes, (2) to evaluate the role of nearshore processes (tidal range, wave climate, record of fair weather vs. high-energy episodic/storm conditions) on deposition, and (3) to reconstruct the coastal morphology and position.

* Corresponding author, e-mail: slavek@sci.muni.cz

Received: July 18, 2022; accepted: October 10, 2022; first published online: December 29, 2022

GEOLOGICAL SETTING

The study area with the exposures investigated is located in northeastern Austria at the southeastern margin of the Bohemian Massif, at the contact with the Alpine-Carpathian Foredeep.

The basement consists of Precambrian crystalline rocks overlain by Lower Miocene (Lower Burdigalian/Eggenburgian to Ottnangian) deposits. In some areas, Pleistocene loess, loam, and solifluction deposits may cover both (Fig. 1A).

The crystalline basement in this area belongs to the Moravian Superunit. It consists of Precambrian (Neoproterozoic) metamorphic rocks, such as paragneiss, mica schist, quartzite, marble and calc-silicate gneiss, which were intruded in the late Neoproterozoic by different granites and granodiorites. In the area described here, the Retz granite of the Thaya Batholith forms the southeastern margin of the Bohemian Massif. In the west it intrudes mica schist and quartzite, which alternate with various gneisses (Therasburg gneiss, Weitersfeld gneiss; Roetzel et al., 1998, 1999a). The crystalline margin is formed by a NE–SW trending sinistral fault-system, including the Diendorf fault and the Waitzendorf fault (Roetzel, 1996; Fig. 1), which are normal faults where the Miocene strata have been vertically displaced by up to 100 metres.

East of the Waitzendorf fault, a crystalline elevation runs between Retz and Zellerndorf, where the granite protrudes from the sedimentary cover in numerous crystalline islands. This crystalline uplift is dissected by several N–S striking faults that form a tectonically induced horst-graben topography (Roštínský and Roetzel, 2005).

Between the Waitzendorf fault and this crystalline uplift, the Obermarkersdorf Basin subsided, in which Lower Miocene sediments of the Eggenburgian and Ottnangian were deposited (Schubert et al., 1999). The basin is bounded by crystalline rocks to the west, north and east and opens to the south, where it extends to the Pulkau River.

In the Lower Miocene strata of the area between Eggenburg and Retz two distinct transgressive sequences with several lithostratigraphic units can be distinguished (Roetzel et al., 1999b; Mandic and Steininger, 2003; Piller et al., 2007). The first marine transgression, which began in the early Eggenburgian, reached this area in the late Eggenburgian with deposition taking place directly above the crystalline basement. In the study area, the deposits of the Burgschleinitz Formation in particular are associated with this cycle.

Strata of the Burgschleinitz Formation are found in the study area at the surface mainly at the northern margin of the Obermarkersdorf Basin (Fig. 1), where the exposures described in this paper occur in the Diem sand pit and in the area of Rosenau (see Figs. 2 and 3).

The deposits of the Burgschleinitz Formation are mainly variously sorted, partly gravelly fine-, medium- and coarse-grained sands with intercalations of angular to subrounded, sandy fine to coarse gravel, cobbles and boulders. Towards the crystalline margin, such as in the vicinity of Rosenau, the sand-rich facies of the Burgschleinitz Formation laterally interfingers with high-energy cobble and boulder facies. These strata were partially deposited in several metre-deep pockets of the crystalline basement, whose surface has been rounded, smoothed and polished by marine erosion. Erosional relics of the sands with intercalated boulder layers are also found further west, in a somewhat higher position overlying granite of the Thaya Batholith (Fig. 1B).

The Burgschleinitz Formation in the Obermarkersdorf Basin has a thickness of at least 20 metres. In contrast to the Burgschleinitz Formation in the Eggenburg Bay (Nehyba and Roetzel, 2021), the deposits are here very poor in fossils. Bivalves, fish teeth and ribs of sea-cows are found only rarely (Roetzel and Heinrich, 1999).

The second transgressive cycle starts with the Zogelsdorf Formation (Nebelsick, 1989), which was deposited in the early Ottnangian, at the beginning of a new marine ingression into the area (Piller et al., 2007). A distinct hiatus and pronounced erosional relief, due to the drop in sea level and regression around the Eggenburgian-Ottnangian boundary, mark the base of this formation.

The calcareous sandstones and fossiliferous limestones of the Zogelsdorf Formation are mainly distributed in the Eggenburg Bay (Nebelsick, 1989). Outside the Bay, they are found in the vicinity of Pulkau and in the southern Obermarkersdorf Basin, as well as along the Pulkau River and other brooks west of Zellerndorf (Fig. 1A). How far they extend subsurface northwards in the Obermarkersdorf Basin is not known.

The Zogelsdorf Formation in this area lies above the Burgschleinitz Formation or on crystalline basement. It consists of basal conglomerates, poorly sorted and silty coarse to medium-grained sands, sandstones, as well as coralline algal and bryozoan detrital limestones (Nebelsick, 1989). Originally aragonitic mollusc shells are always entirely diagenetically leached, while calcitic ones remain.

The Zogelsdorf Formation is a fining and deepening upwards succession, which passes upsection into open marine clays and marls of the Ottnangian Zellerndorf Formation. In most cases, the transition is within a metre-thick, poorly sorted and gravelly to coarse sandy silt to clay.

The majority of the Zellerndorf Formation consists of finely laminated and thin-bedded, light- and dark-brown or bluish-grey, mostly non-calcareous and smectitic, very fine-grained silty clays. The pelites of the Zellerndorf Formation are predominant close to the surface, especially in the Obermarkersdorf Basin and in the Zellerndorf area (Fig. 1A). Due to the rapidly progressing early Ottnangian transgression, direct onlap of the pelitic facies onto crystalline elevations locally occurs, especially on the ridge north of Zellerndorf.

North-east of the Obermarkersdorf Basin, especially in the vicinity of Retz, 20- to 60-m-thick, predominantly coarse- to fine-grained sands of the Retz Formation occur (Roetzel et al., 2005). The Retz Formation comprises generally medium- to fine-grained sands, in places with layers of coarse-grained sand, fine gravel, and intercalations of granite pebbles. In the vicinity of bedrock elevations, gravelly medium- to coarse-grained sands and granite pebbles and cobbles up to 15 cm across occur. In some areas, the sands are irregularly concretionary consolidated and partly fossiliferous.

Generally, these deposits are lithologically comparable to the Burgschleinitz Formation. However, intercalations of calcareous sandstone and fossiliferous limestone as well as indicative fossils, such as a diverse bryozoan fauna (Kühn, 1955; Vávra, 1979, 1981) or the occurrence of *Pecten hornensis* and *Gigantopecten holgeri* allow correlation of most of the Retz Formation with the Zogelsdorf Formation (Mandic and Harzhauser, 1999; Roetzel et al., 1999b). Nevertheless, it is likely that parts of the Retz Formation were already deposited in the late Eggenburgian and correlate with the Burgschleinitz Formation due to their similar lithology. In some areas, however, the sands interfinger also laterally with the Zellerndorf Formation.

Despite the lack of boreholes in the central part of the Obermarkersdorf Basin, geophysical investigations (Schubert et al., 1999) indicate that deposits of the Burgschleinitz Formation and Zogelsdorf Formation are also developed beneath the Zellerndorf Formation within the basin. In the southern part of

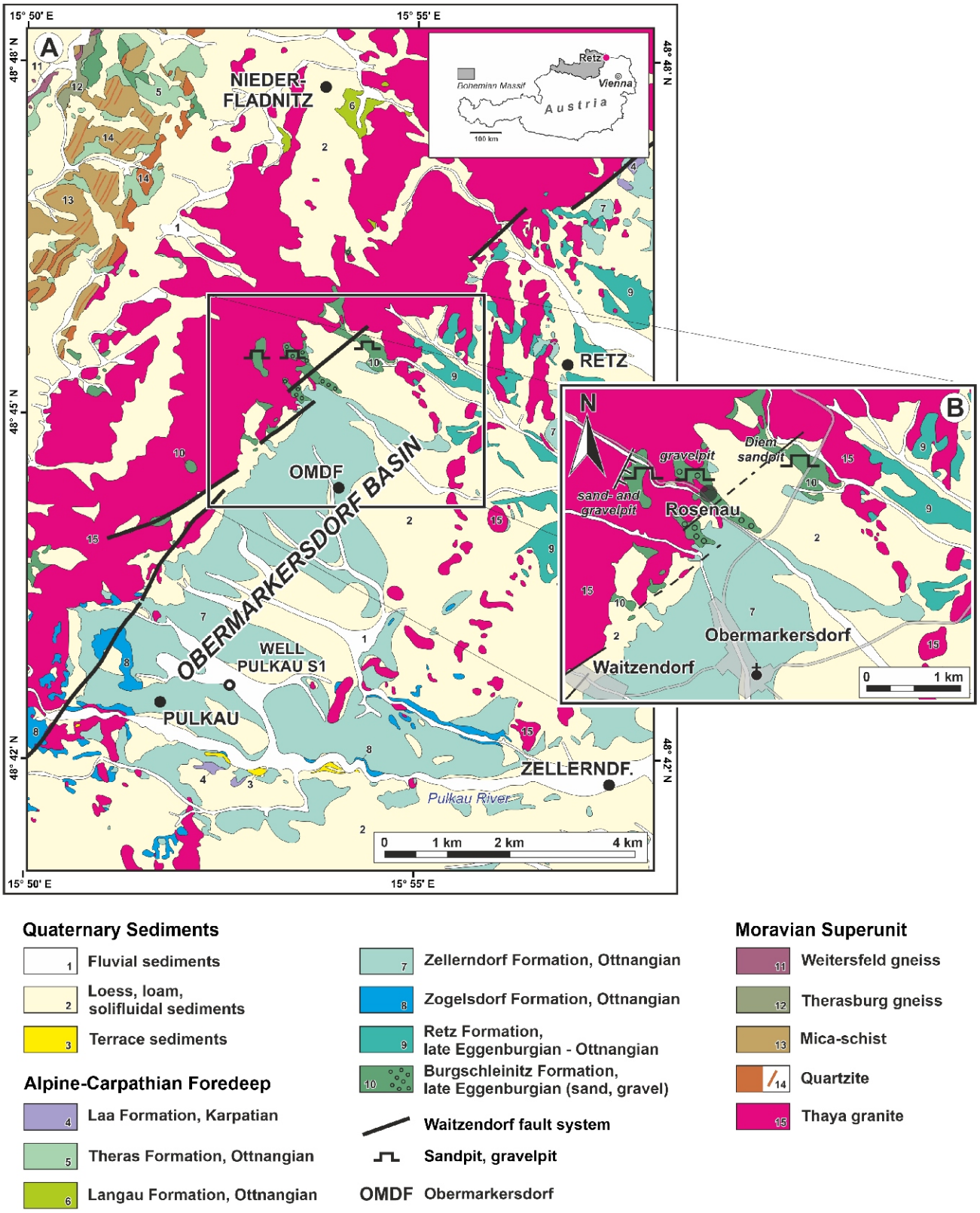

Fig. 1A – geological map of the surroundings of the Obermarkersdorf Basin; B – detailed geological map with location of the exposures investigated near the villages of Obermarkersdorf and Rosenau (from Roetzel et al., 1998, 1999)

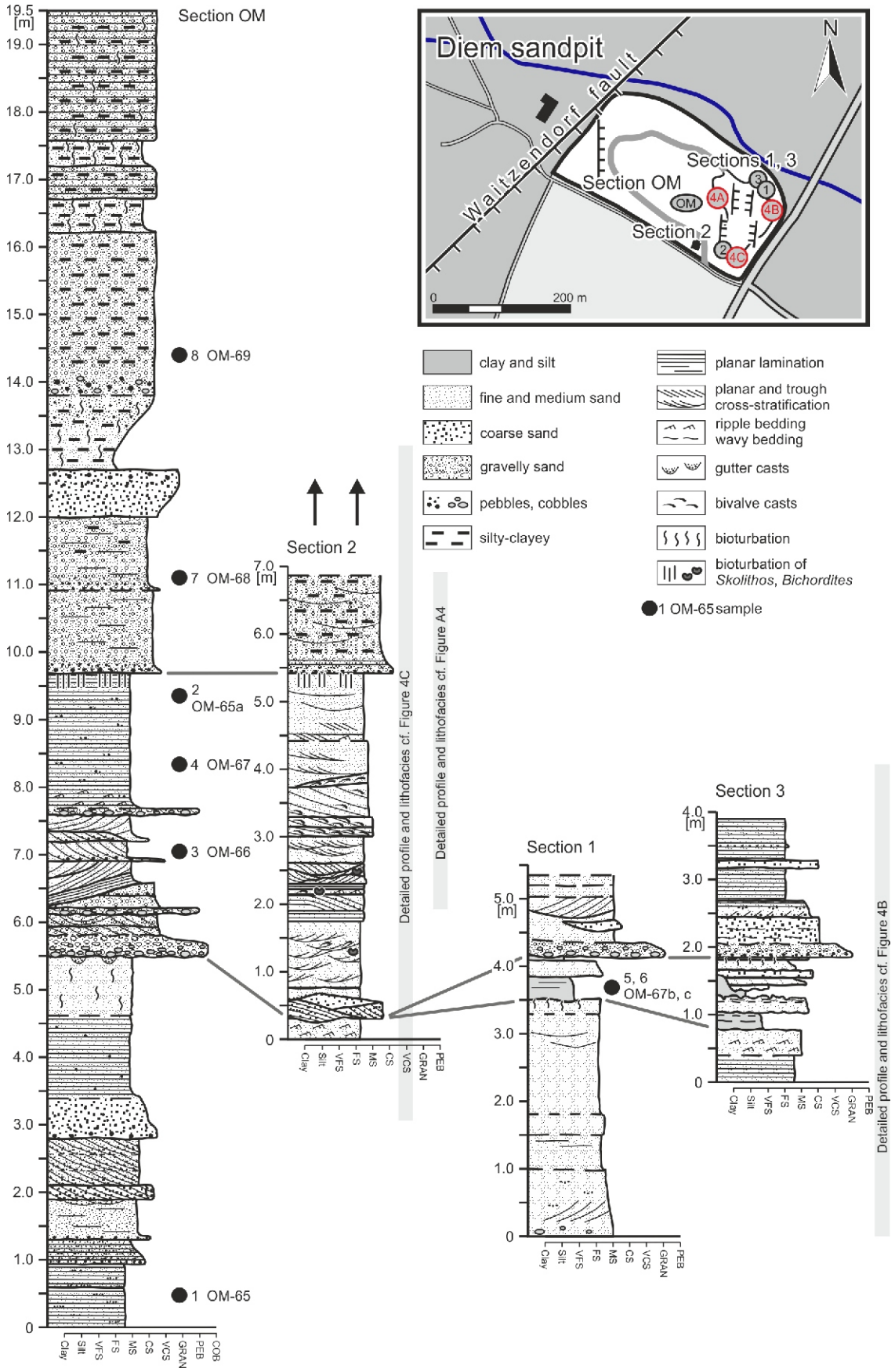

Fig. 2. General section OM, sub-sections 1–3 and exposure situation in the area of the Diem sand pit

The sections/logs OM and 1–3 are marked in the map; sidebars and red circles in the map refer to sections/logs in Figure 4A–C

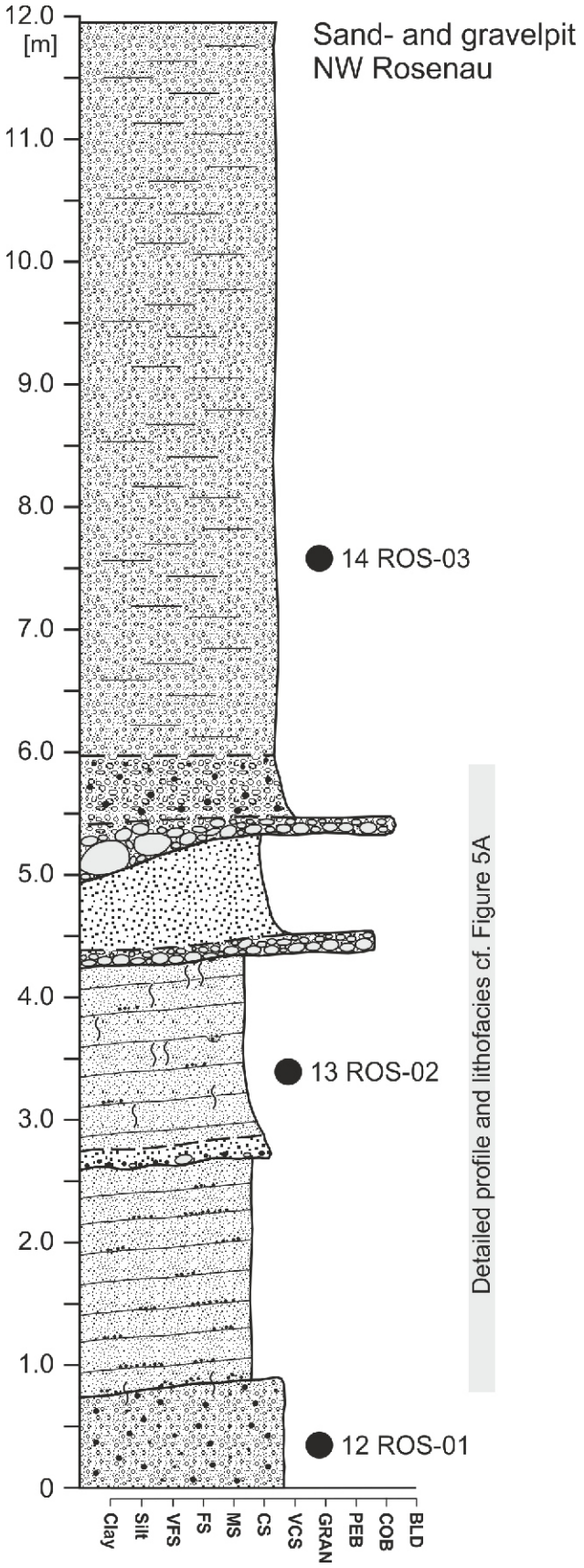

Fig. 3. General section of the sand and gravel pit NW of Rosenau, west of the war memorial

Sidebar refers to section/log in Figure 5A

the basin, north of Pulkau, a nearly 55 m deep borehole in the Teichgraben (Roetzel in Schubert et al., 1999; Fig. 1A) shows the complete sedimentary infill of the basin. Above the slightly weathered granite the sedimentary succession starts with ~16 m of mainly gravelly medium- to coarse-grained sands with silty and fine sandy intercalations of the Burgschleinitz Formation from the first marine transgression in the late Eggenburgian. Above, a ~4.5 m thick pelitic inteval with a brackish fauna and small tuffitic intercalations indicates the regressive phase at the base of the Ottnangian. It is followed by ~18 m of poorly sorted and very silty coarse- to fine-grained sands, which are very often lithified to calcareous sandstone. These deposits of the Zogelsdorf Formation mark the start of the next marine transgression in the early Ottnangian. The uppermost, ~10 m-thick part of the sequence is formed by silty clays of the Zellerndorf Formation which show the further landward ingression of the sea.

METHODS

Fieldwork was based on detailed logging, drawing of bedding architecture and photomosaics and measurement of palaeocurrent indicators (see Collinson et al., 2006) in exposure walls close to Obermarkersdorf (Diem sand pit) and Rosenau. Primary sedimentary structures and textures were used for distinguishing the lithofacies (Walker and James, 1992). Lithofacies were grouped into facies associations (FAs), i.e., assemblages of spatially and genetically related facies that are expressions of different sedimentary environments. These FAs are labelled with interpretive genetic names for convenience, but their descriptions are separated from interpretations in the text.

Grain size analyses of samples were done by wet sieving with a *Retsch AS 200* sieving machine at 1 intervals for fractions >0.063 mm. Pelitic samples were sieved at $^{1}/_{2}$ intervals and the fractions <0.063 mm were analysed at the Austrian Geological Survey by a *Micromeritics SediGraph 5000 ET* down to 2 μm and at the Masaryk University in Brno (three samples) with a *Cilas 1064* laser diffraction granulometer down to 0.4 μm. Utrasonic dispersion, distilled water and washing in sodium polyphosphate were used prior to analyses to avoid flocculation of the particles analysed. The mean grain size is representated by the graphic mean (Mz) and the uniformity of the grain size distribution/sorting by the standard deviation (I) (Folk and Ward, 1957).

Pebble and cobble petrography, shape and roundness were determined either visually in the exposures (gravelly facies) or under the microscope, determining the coarsest portion (clasts larger than 1.6 cm) of the sandy facies. Shape and roundness were estimated visually using the shape classification of Zingg (1935) and Powers (1953). The maximum pebble/cobble size represents an average of the longest axis (A-axis) of the 10 largest extraclasts found at a locality. Clast assemblages were evaluated *sensu* Bluck (1999).

For provenance analyses of the sands, evaluation of both light and heavy minerals was used. Light minerals of the 0.063–0.425 mm fraction from 6 samples were embedded in synthetic resin and, after curing and preparation of thin sections, evaluated under a polarising microscope (more than 300 grains each sample). Heavy minerals from 7 samples were separated with tetrabromoethane and, after preparation in strew slides, also quantified in the 0.063–0.425 mm grain size fraction under a polarising microscope by counting. The opaque and translucent minerals were considered separately.

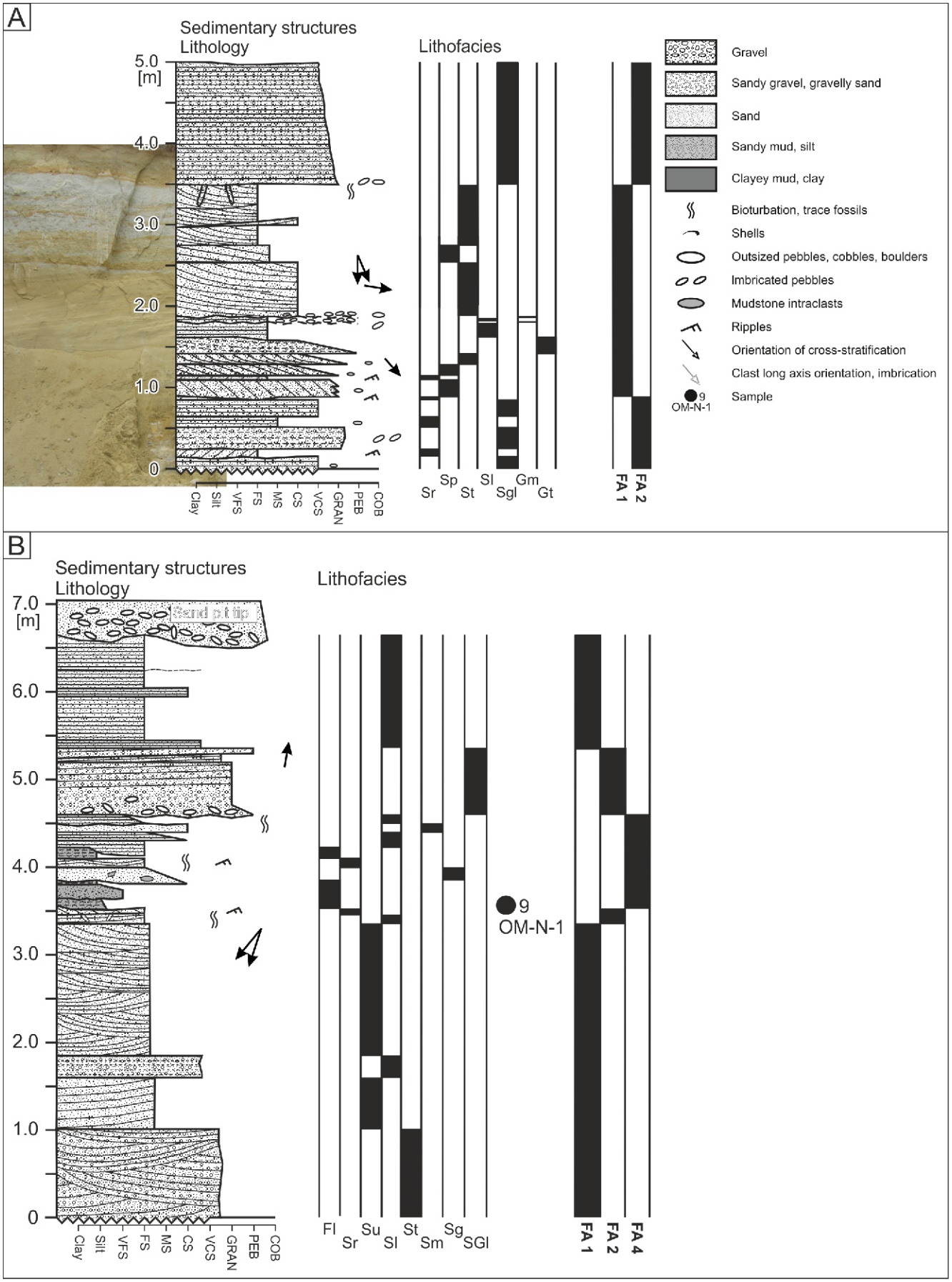

Fig. 4. Schematic lithostratigraphic sections of the Diem sand pit

A – Diem I – log of the NW wall; **B** – Diem II – log of the NE wall; **C** – Diem III – log of the SE wall with distribution of facies associations (FAs); for position of sections refer to Figure 2

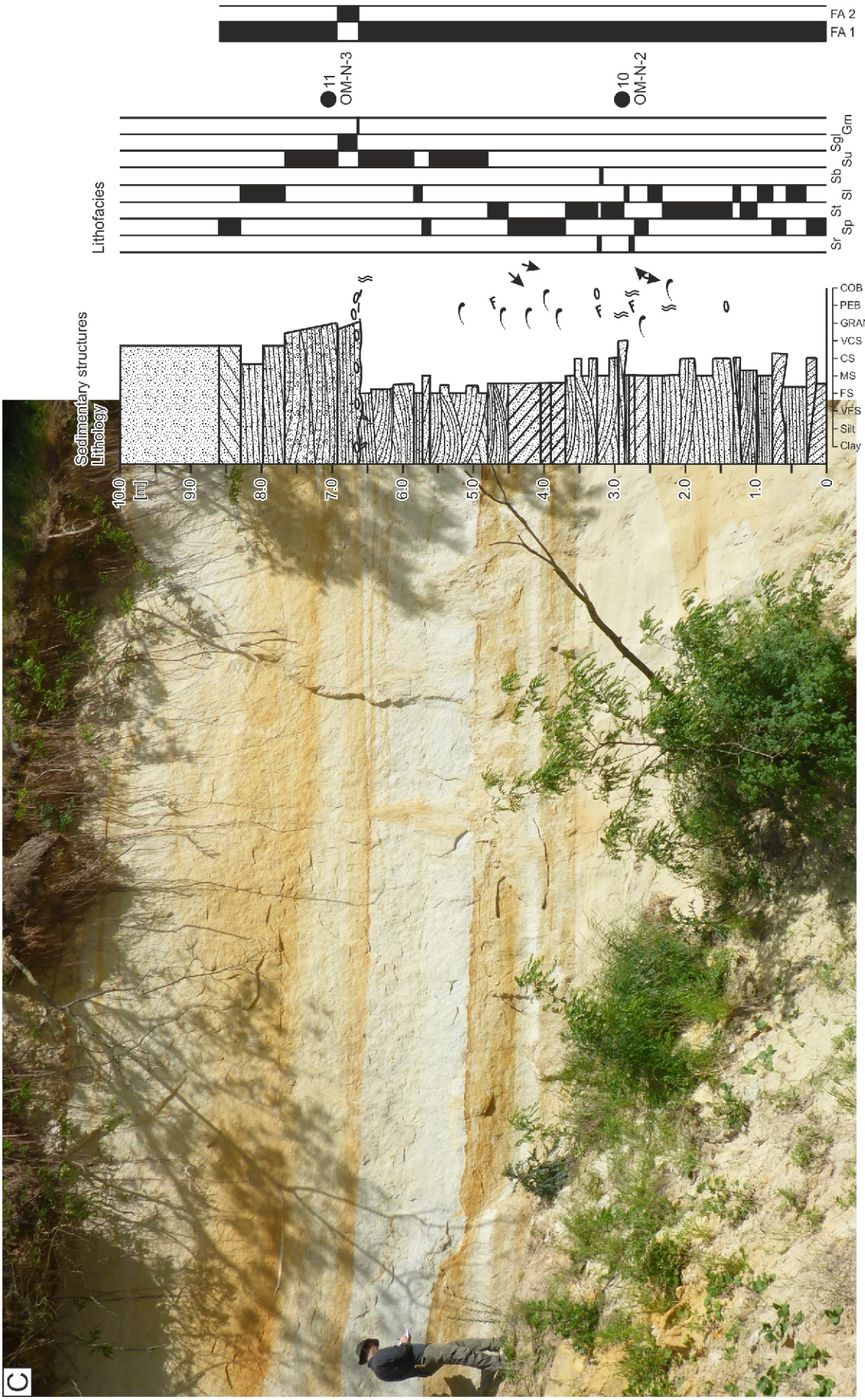
C
FA 2
FA 1
11
OM-N-3
10
OM-N-2
Lithofacies
Gm
Sg
Su
Sb
Sl
St
Sp
Sr
Sedimentary structures
Lithology
COB
PEB
GRAN
VCS
CS
MS
FS
VFS
Silt
Clay
10.0
[m]
9.0
8.0
7.0
6.0
5.0
4.0
3.0
2.0
1.0
0

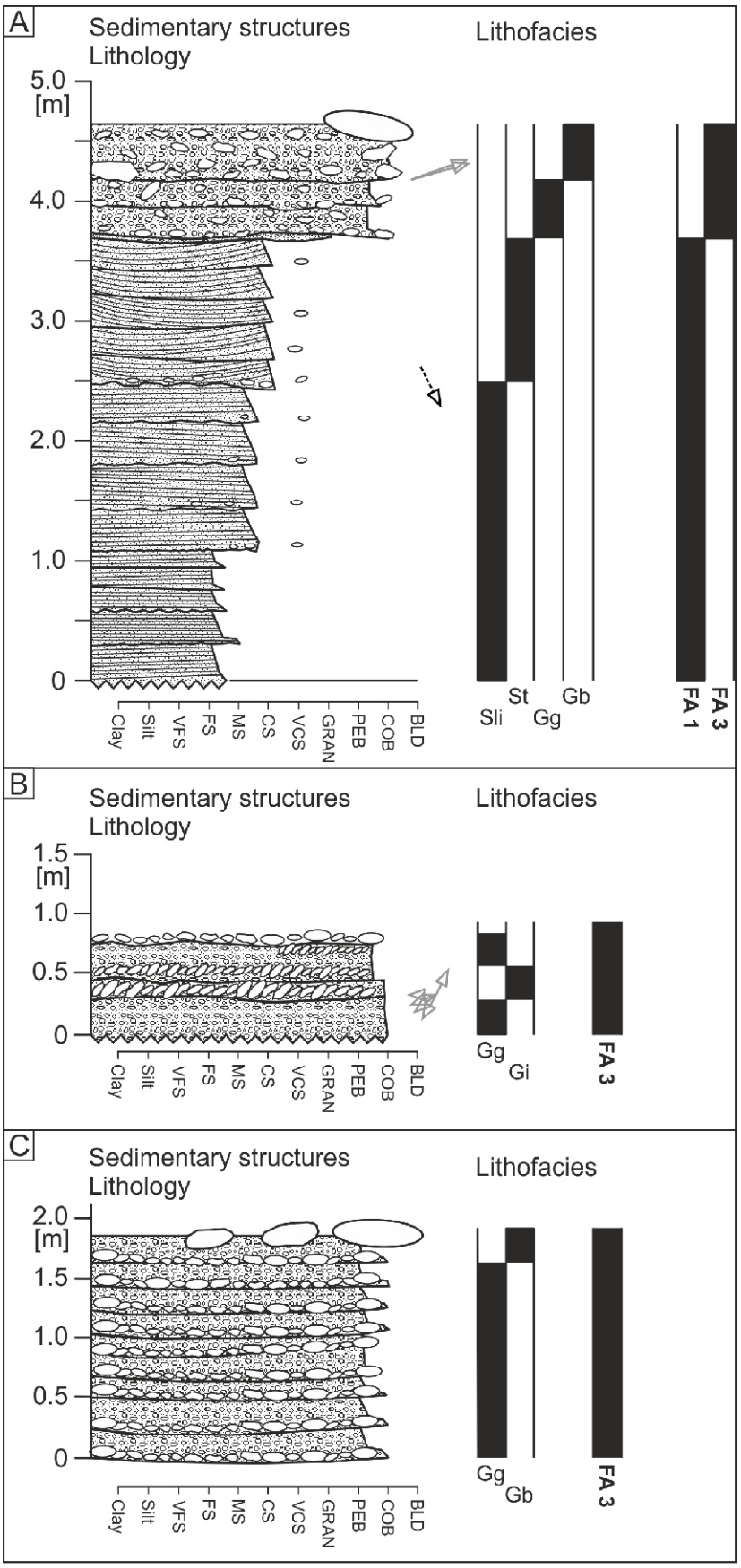

Fig. 5. Schematic lithostratigraphic sections of the Rosenau sand and gravel pits

A – log of the sand and gravel pit NW of Rosenau, west of the war memorial "Schrattenthal sand pit", for position of section refer to sidebar in Figure 3; **B** – log of the lower portion of the gravel pit NW of Rosenau "Pfarrgrube"; **C** – log of the upper portion of the Rosenau gravel pit "Pfarrgrube" with distribution of facies associations (FAs); explanations as in Figure 4

The chemistry of garnet was analysed in 35 grains; the chemistry of rutile was based on data from 8 grains. All grains were randomly chosen. Electron microprobe analysis was done on a *CAMECA SX* electron microprobe analyser (Faculty of Science, Masaryk University, Brno). Measurements were carried out under the following conditions: wave propagation mode, accelerating voltage 15 keV, beam current 20nA, beam size 2 µm. Garnets were checked for internal zoning. Because the grains examined did not display chemical zoning, the chemical composition was examined in single spots located in grain centres. Zircon studies (external morphology, colour, presence of older cores, inclusions and zoning, elongation) were carried out on 247 grains from 5 samples (grain size fraction 63–125 µm). Results of zircon typology (Pupin, 1980) are based on 52 euhedral crystals and its elongation on 75 unbroken grains. Chemical analysis of three zircon grains was also available.

RESULTS

SECTION DESCRIPTIONS

The sedimentary succession of the Lower Miocene deposits was mainly studied in the large Diem sand pit, 2.3 km NNE of the village of Obermarkersdorf (N48°45'33", E15°54'24", 300 m a.s.l.; Figs. 2 and 4). Studies of coarse gravely deposits were made in an abandoned gravel pit "Pfarrgrube" 350 m north-west of the village of Rosenau (N48°45'29", E15°53'22", 385 m a.s.l.) (Figs. 3 and 5B, C) and in an abandoned sand and gravel pit ("Schrattenthal sand pit") 500 m west, on the opposite side of the valley, west of a war memorial (N48°45'31", E15°52'56", 403 m a.s.l.; Figs. 3 and 5A). The locations of the exposures investigated are shown in Figure 1B and the geological map of the area investigated in Figure 1A.

In the Diem sand pit, on the northern edge of the Obermarkersdorf Basin, shallow marine deposits of the Burgschleinitz Formation are exposed in a ~20 m-thick sandy section (Roetzel and Heinrich, 1999). With the exception of bioturbation, these sands are largely unfossiliferous. However, rare fossils such as bivalves, fish teeth and ribs of seacows as well as typical sedimentary structures indicate a shallow marine depositional environment.

Additionally, in the uppermost part, at the western edge of the pit, close to a normal fault, Quaternary, reddish-brown loam (?palaeosol sediments) was exposed in the past.

The sand pit is located near the north-east–south-west trending Waitzendorf fault (Fig. 1). The sands in the pit are affected by several north-south striking, east- and west-dipping steep faults with offsets of up to 10 m. Especially in the eastern part of the pit, these faults formed a tight network of horst-graben structures (Fig. 2).

A complete profile of the section is described below from the central part of the sand pit; however, this is no longer completely exposed today (Fig. 2, section OM). In addition, three sub-profiles are shown from the eastern part of the sand pit, which differ somewhat in lithology and facies from the main profile (Fig. 2, sections 1–3). They show the lateral variation of lithology towards the south-east and east depending on the distance from crystalline elevations.

In the main section (Fig. 2, section OM) the basal, ~5.5 m-thick sedimentary part, is formed mainly of well- to moderately sorted, fine- and coarse-sandy medium-grained sands. It consists of 20 to 60 cm-thick sedimentary units, that show predominantly mm-thick planar lamination, in some cases also cross-stratification and in places normal grading.

Above this follows a ~2.2 m-thick, coarse-grained part. It consists of fine-gravelly coarse sands with three intercalated pebble and cobble horizons. Planar- to cross-stratified dunes of fine-sandy medium-grained sands are intercalated between them.

In the hanging wall of the coarse-grained part follow well-sorted and medium- to fine-grained sands, which are mainly planar bedded. The thickness of these sands increases significantly towards the east, from ~2 to ~5 m. Traces of the *Skolithos* ichnofacies with escape structures are present at the top of this layer.

In contrast to the lower part of the section, the deposits in the ~10 m-thick upper part are clearly different. Poorly sorted, silty, mostly fine-gravelly, coarse- and medium-grained sands predominate here. The deposits are divided into 50 to 240 cm-thick units, which are indistinctly stratified or in some cases completely massive due to intense bioturbation. They include a high proportion of lithic components from granite.

In the northeastern part of the sand pit, a 0.6 to 1.5 m-thick sandy and pelitic sequence is intercalated laterally to the basal part of the sedimentary package described above (Fig. 2, sections 1 and 3). It pinches out towards the east and south and probably interfingers with the coarse-grained, gravelly and pebbly part of the main section. Planar laminated greyish and whitish-grey clayey silts alternate sharply with dm-thick layers of yellowish-brown fine, medium and coarse sands. The sands often are fining upwards and convolute stratification is developed in contact with the pelitic layers. In the clay fraction of these pelites kaolinite and fireclay predominate at ~81%. The proportion of smectite, on the other hand, is low at ~19% (Roetzel and Heinrich, 1999).

In the southeastern part of the sand pit, the middle part of the main section is exposed, which was thrusted down in a tectonic graben along north-south striking normal faults (Fig. 2, section 2). In this section, only one basal gravelly horizon is exposed, overlain by a nearly 5 m-thick sequence of fine- to medium-grained sands. These sands show multiple alternations of planar and trough cross-stratification, interrupted by thinner horizons with planar lamination and ripple stratification. Disarticulated shell casts of bivalves occur in the middle part of this profile, aligned parallel to the cross-stratification. The majority of the shell casts have a stable convex-upwards position. In addition, dwelling-traces of sea urchins (*Bichordites*) occur in the sands. Below the poorly sorted coarse sands in the hanging wall traces of the *Skolithos* ichnofacies occur.

In the abandoned sand and gravel pit north-west of Rosenau, south of the road to Weitersfeld, west of a war memorial, (Figs. 1B and 3), sands with gravelly intercalations were preserved as erosion relicts in the Thaya Batholith in an orographically significantly higher position than in the Diem sand pit. In the western part of the sand pit, a steep NNE–SSW striking fault with an offset of ~2 m towards ESE cuts the sands.

The ~12 m-thick section starts at the base with ~1 m of fine gravel in a coarse- to medium-grained sandy matrix. The coarse fraction is dominated by angular to subangular granitic components. Above, 3.5 m of planar-stratified and coarse-sandy medium-grained sands follow. The deposits have thin, coarse-sandy interbeds on the bedding planes and are divided by a dm-thick, coarse-grained layer with a few granite pebbles. The upper part is also more bioturbated and locally shows gutter casts.

This is followed by a very coarse interval with granite cobbles and boulders. In the northwestern part of the pit this layer is up to 1.3 m thick. Towards the south, an up to 80 cm-thick coarse- to medium-grained sand layer is intercalated within the

coarse clastic deposits, indicating multiphase deposition. The cobbles and boulders in a sandy matrix are mostly 5–20 cm in diameter, but in rare cases can reach up to 1 m in size. They are well-rounded to subrounded, and the larger blocks also subangular to angular.

The uppermost part of the section consists of relatively uniform fine-gravelly coarse- to medium-grained sands. These are indistinctly planar-stratified and consist in the coarse fraction mainly of lithic fragments (mainly from granite). Sorting of the sands is slightly worse than in the sands below.

In the abandoned gravel pit "Pfarrgrube" 350 m north-west of Rosenau, north of the road to Weitersfeld (Fig. 1B), only very coarse deposits from pebbles to boulders are exposed. The deposits follow directly above the granite of the Thaya Batholith which shows a strongly pronounced relief. Pockets between several metres-high granite elevations are filled with coarse gravel, most of which is only very indistinctly stratified.

The gravelly sequence is up to 8-m-thick. Pebbles and cobbles are mostly subrounded to subangular, some large boulders are also well rounded. The components have mainly diameters of 5–15 cm, larger boulders 20–50 cm. However, granite blocks of 1–2 m across were also observed. Components are spherical to discoidal, with the discoidal ones tending to predominate. Discoidal components are usually adjusted with the longitudinal axes parallel to the stratification. However, imbrication can also be observed.

The coarse components, mainly of quartz-rich, fine-grained rocks, are relatively fresh and unweathered. In contrast, feldspar-rich, coarser-grained granite boulders are often more strongly weathered. The coarse components are mainly clast-supported. The matrix consists of poorly sorted and subangular medium to coarse sand or fine gravel.

FACIES ANALYSIS

Seventeen lithofacies have been recognised and organised into four facies associations (FAs). These FAs are: (1) upper-shoreface deposits, (2) foreshore deposits, (3) gravelly beach deposits and (4) backshore – lagoonal deposits. Detailed descriptions (lithology, stratification and sedimentary structures) and interpretation of each facies recognised are given in Table 1. Logs and line drawings, illustrating the distribution of facies associations at the exposures, are shown in Figures 4 and 5. Examples of lithofacies and facies associations within the logged sections are shown in Figures 6 and 7.

FA 1 – UPPER-SHOREFACE DEPOSITS

Facies association 1 includes ten lithofacies (Sb, Sr, Sp, St, Sl, Su, Sg, Sc, Gr, and Gt), but, only four of them (Sp, St, Sl, and Su) form the volumetrically largest part of the succession, together forming >90% of the measured thickness of FA 1. The rest of the lithofacies forms only thin and/or rare interbeds (Figs. 4 and 5). The vertical thickness of FA 1 varies between 150 and 620 cm in the individual sections; however, its base is not exposed, so its true thickness is significantly higher. FA 1 is usually overlain by FA 2, although, it is also overlain by FA 3. The contact with the overlying FA 2 is sharp, erosive and generally undulose with dm-scale relief. The topmost part of FA 1 is typically bioturbated (*Skolithos* ichnofacies – Fig. 6A). FA 1 was also recognised above FA 2 (see Fig. 4).

The cross-stratified beds of lithofacies St and Sp show complex internal structure, being cut by several second-order surfaces, and contain subordinate interbeds of facies Sr and rarely Sb. Lithofacies St consists of sets of trough cross-stratified, usually fine to medium sand. The set thickness is usually 20–30 cm. Coset thickness is up to 150 cm. Clayey intercalations were not observed. Bioturbation is mostly absent or occurs sparsely in the uppermost part of facies St (contact with FA 2). Lithofacies Sp consists of sets of planar cross-stratified, mostly fine to medium sand. Individual sets could be laterally traced for several metres. Cosets reach a thickness of up to 80 cm and sets are from 15 to 20 cm thick. Coset bounding surfaces are subhorizontal to inclined. The lower contacts are usually erosive, rarely with outsized small pebbles or granule lags. Set bounding surfaces range from horizontal to inclined (up to 20°). Sets and cosets are either uniform in grain size or show a fining upwards trend. Foreset angles of both St and Sp facies vary between 15 and 30°. The directions of palaeocurrents are variable, with a dominance towards SW or SE.

Lithofacies Sl consists of fine-, fine- to medium-, and medium-grained sands, that are well-sorted and subhorizontal or inclined planar parallel-laminated. Bed thickness varies between 10 and 100 cm. Bases are usually sharp, flat horizontal, or inclined; rarely the base is convex down. Planar laminae are oriented subparallel to inclined set-bounding surfaces. Tabular to wedge-shaped beds of lithofacies Sl either separate cosets of lithofacies Sp or St, or there is a lateral transition from subhorizontal laminae (Sl) into inclined foresets (mostly Sp) (Fig. 6B, D, E). Lithofacies Sp, St, and rarely also Sl were observed in two variants, in which bivalves are either common or absent. The shells of bivalves are replaced by limonite and appear as brownish outlines in the sediment. The shell size of the indeterminable but taxonomically clearly unifom bivalves ranges from 2 to 4 cm. A lack of bivalves was observed in the lower part of the succession while they occur in its upper part (see Fig. 6F, H). Sands without bivalves are relatively well-sorted, and shelly sands are poorly sorted. Foresets (Sp, St) in particular are often traced by the alignment of bivalves parallel to the inclined laminae. The open, disarticulated shells show a predominantly stable, convex-up position.

Lithofacies Su consists of fine- to medium- and medium- to coarse-grained sands with broad, concave-up laminae parallel to shallow broad concave-up basal surfaces/scours (see Fig. 6F). Concave-up laminae dip at low angles. Bed thickness varies between 15 and 80 cm. Lithofacies Su was found mainly in the upper part of FA 1 and is generally well-sorted, although rare bivalves and/or small granite or quartz pebbles may be present. A fining upwards trend is common in Su beds.

Lithofacies Sr forms isolated lenses and thin layers of rippled, relatively well-sorted, fine- to medium-grained sands (see Fig. 6C). Beds of facies Sr show predominantly erosional tops, while bioturbation, outsized clasts or shell fragments were not observed.

Lithofacies Sb forms only isolated erosional relics of generally lensoid shape, max. 6 cm thick. The lack of preserved physical sedimentary structures is due to high bioturbation intensity.

An isolated, medium thick bed of lithofacies Sc consists of fine-grained, well-sorted sand. It shows convolute stratification evolving towards the top of the bed from uneven planar parallel lamination close to the base. The bed is wedge-shaped.

Another isolated, medium thick bed of lithofacies Gt consists of matrix- to clast-supported pebble gravel and is trough cross-stratifed. Pebbles are from granites and quartz and rounded to subrounded. The tabular to wedge-shaped bed shows a crude fining upwards trend.

The occurrence of lithofacies Gr is important. These gravelite to pebble gravel beds are massive or small-scale cross-stratified and form isolated convex-up bedforms with flat, planar basal surfaces (see Fig. 6C). Undulose tops with rounded crest profiles are typical. The crests appear to be regularly spaced in some cases (with amplitudes of ~10 cm). A gen-

Table 1

Brief description and interpretation of lithofacies in the studied profiles of the Burgschleinitz Formation

Symbol	Description	Interpretation
Gb	Cobble gravel, clast supported to openwork. Massive, no imbrication, sometimes clast shadows. The spaces between the larger clasts are filled with smaller ones or even with coarse sand. Pebbles, cobbles and boulders (90 cm in diameter) are mostly rounded, rarely subangular. No significant shape sorting. Boulders, cobbles and pebbles are mostly rods, spheres or blades. Discs seem to be present in relative smaller amounts. Bed thickness 24–40 cm.	Wave and current activity in the subaqueous zone (Bluck, 1967; Postma and Nemec, 1990)
Gg	Cobble to pebble gravel, openwork to clast supported, massive to crudely subhorizontal stratification. The base of the bed is formed by large pebbles, cobbles and rarely even boulders (max. 30 cm in diameter), which are lying flat (A-axis parallel) along the base. These clasts are mostly blades or spheres. This basal "lag" is covered by progressively finer pebbles and rare floating cobbles (coarse tail normal grading), openwork to clast supported, pore-space might be filled with substantially smaller clasts. The pebbles are mostly rods and spheres, however, blades and discs were also identified. Preferred orientation of pebbles and pebble shape separation are missing. Pebbles and cobbles are mostly rounded, subangular ones are rare. Bed thickness 15–25 cm. Sharp flat or broadly undulose base. Top is sharp, broadly undulose, erosional.	Wave and current activity along the beachface (Bluck, 1967; Postma and Nemec, 1990)
Gi	Pebble to cobble gravel. Relatively outsized cobbles (max. 15 cm in diameter) and large pebbles aligned parallel along the base. Higher imbricated progressively finer pebbles (mostly ~5–6 cm in diameter) and some cobbles. Pebbles and cobbles are mostly blades, rarely discs or rods. Clast supported to openwork, locally space infilled with coarse sand. Sharp to broadly convex/concave upwards (undulose base). Sharp uneven erosive top. Bed thickness 15–26 cm.	Wave and current activity in the higher subaqueous zone of a beach (Bluck, 1967; Postma, Nemec, 1990)
Gm	One to a few pebbles thick bed of flat lying rounded to well-rounded pebbles, up to 6 cm in diameter. Subhorizontal undulated and locally discontinuous beds with very unstable thickness (max. thickness 6 cm). Erosive undulated base, irregular shape of transitional top (if lithofacies SGl in superposition).	Pebble lag produced by winnowing action of waves
Gt	Matrix to clast supported pebble gravel, trough cross-stratification. Set thickness of ~20 cm, coset ~40 cm, crude fining upwards trend. Erosive convex down base. Pebbles with rare cobbles (up to 10 cm) enriched along the base. Sharp flat broadly undulated top. Pebbles are mostly formed by quartz and granitic rocks, rounded to subrounded. Tabular to wedge-shaped bed.	Unidirectional tractive flow giving rise to 3D dune bedforms
Gr	Gravelite to pebble gravel, matrix to clast supported. Matrix formed by coarse to very coarse sand. Individual beds are structureless, or cross-stratified. Well-rounded pebbles (up to 3 cm in diameter), imbricated to flat lying parallel to the flat erosive base. Crude fining upwards trend of the beds. Sharp planar or slightly inclined base. Almost regularly rounded, undulated top. Inclined, wedge-shaped beds, bed thickness up to 20 cm.	Gravely megaripples formed under oscillatory and/or combined flows
SGl	Poorly sorted coarse to very coarse sand with scattered granules and pebbles to gravelly sand. Planar parallel stratification, locally slightly uneven/undulated. Gravel clasts are angular to rounded. Long axis of pebbles oriented parallel to stratification. Medium to thick bedded (bed thickness 10 to 150 cm). Rare cobles up to 15 cm across along the base. Typically sharp uneven base, erosive. Sharp, flat top.	Result of swash and backwash action on the foreshore. Scattered pebbles and cobbles could represent relics of gravel beds
Sg	Coarse sand along the base of the bed grading upwards into medium to fine sand (distributional normal grading), massive. Scattered irregularly distributed subangular intraclasts of facies Fl up to 3 cm across. Sharp erosive base with relief of several cm, flat gradual top (transitional to bed of facies Sl). Bed thickness 5–15 cm.	Rapid deposition from unidirectional tractive flow
St	Fine, medium to fine, medium to coarse, coarse sand, trough cross-stratified, sometimes bioturbated (subvertical shafts up to 15 cm deep, filled with coarse to very coarse sand, without spreiten, up to 1 cm in diameter – *Skolithos* ichnofacies). Crude fining upwards trend within the bed. Mostly well-sorted sands, sometimes with scattered granules and fine to medium pebbles (up to 1 cm in diameter). Grain size variations between individual sets. Set thickness between 12–30 cm, Coset thickness up to 150 cm. Sharp irregular top.	Unidirectional tractive flows forming 3D dune bedforms. Associated amalgamation and erosive surfaces indicate interaction with waves destroying former bedform (Kern et al., 2019)
Sp	Fine, medium, coarse to very coarse sand with scattered granules, planar cross-stratification. Commonly fining upwards trend within the bed. Set thickness 15-20 cm, coset thickness up to 80 cm. Sharp uneven, inclined or undulated erosive base. Sharp almost flat top. Tabular to wedge-shaped beds.	Unidirectional tractive flows forming 2D dune bedforms
Sr	Fine sand, ripple cross-laminated. Moderately sorted, locally irregularly distributed scattered grains of coarse sand. Bioturbation absent or low index of bioturbation. Sharp slightly undulated or planar subhorizontal base. Irregular erosional top or flat to slightly uneven nonerosive top. Mostly tabular beds, rarely wedge-shaped beds (erosive relics). Bed thickness 3–10 cm.	Action of symmetrical and asymmetrical waves, or action of wave-induced currents
Sl	Fine, fine to medium, medium sand, planar parallel laminated, both subhorizontal to low angle inclined. Relatively well-sorted, sometimes scattered granules and pebbles. Bioturbation absent or low index of bioturbation. Bed thickness 10 to 100 cm. Mostly sharp flat horizontal or inclined base, less common is convex down base. Flat horizontal or inclined top. Tabular to wedge-shaped beds.	Multiple origins: surf assemblage includes planar lamination, surf–swash transition assemblage contains planar lamination
Su	Fine to medium, medium to coarse sand with rare scattered small pebbles. Convex down planar parallel lamination. Fining upwards trend. Bed thickness 15 to 80 cm. Sharp convex down or undulose base, sharp flat top. Tabular bed on the scale of outcrop.	Result of scour-and-fill process of wave action combined with unidirectional currents
Sb	Fine sand, relatively well-sorted, irregular stratification due to bioturbation. Irregularly lensoid bed max. 7 cm thick. Irregular convex down base, transitional generally flat top.	Action of organisms obliterating primary structures
Sc	Fine sand, convolute stratification evolving to the top of the bed from uneven planar parallel lamination close to the base. Well-sorted. Erosive inclined top, flat slightly irregular base. Bed thickness 55 cm. Wedge-shaped bed.	Penecontemporaneous deformation of mainly facies Sl connected with water escape
Sm	Coarse sand, massive, relatively well-sorted. Tabular bed, flat erosive base, flat top, both top and base broadly undulated. Bed thickness 10 cm.	Rapid deposition from unidirectional heavily laden current
Fl	Clayey silt to silty clay, sometimes admixture of very fine sand. Wedge-shape bed, thickness varies from 150 cm to several cm. Erosive relic. Uniform grey colour or in case of thick bed alternation of whitish and greyish layers ~10 to 18-cm-thick. Planar parallel laminated. Sharp, uneven base with relief of several cm. Sharp almost planar to convex down erosive top. Common plastic deformation, especially close to the fault.	Deposition in a protected area, mostly from suspension. Admixture of sand points to distant influence of currents

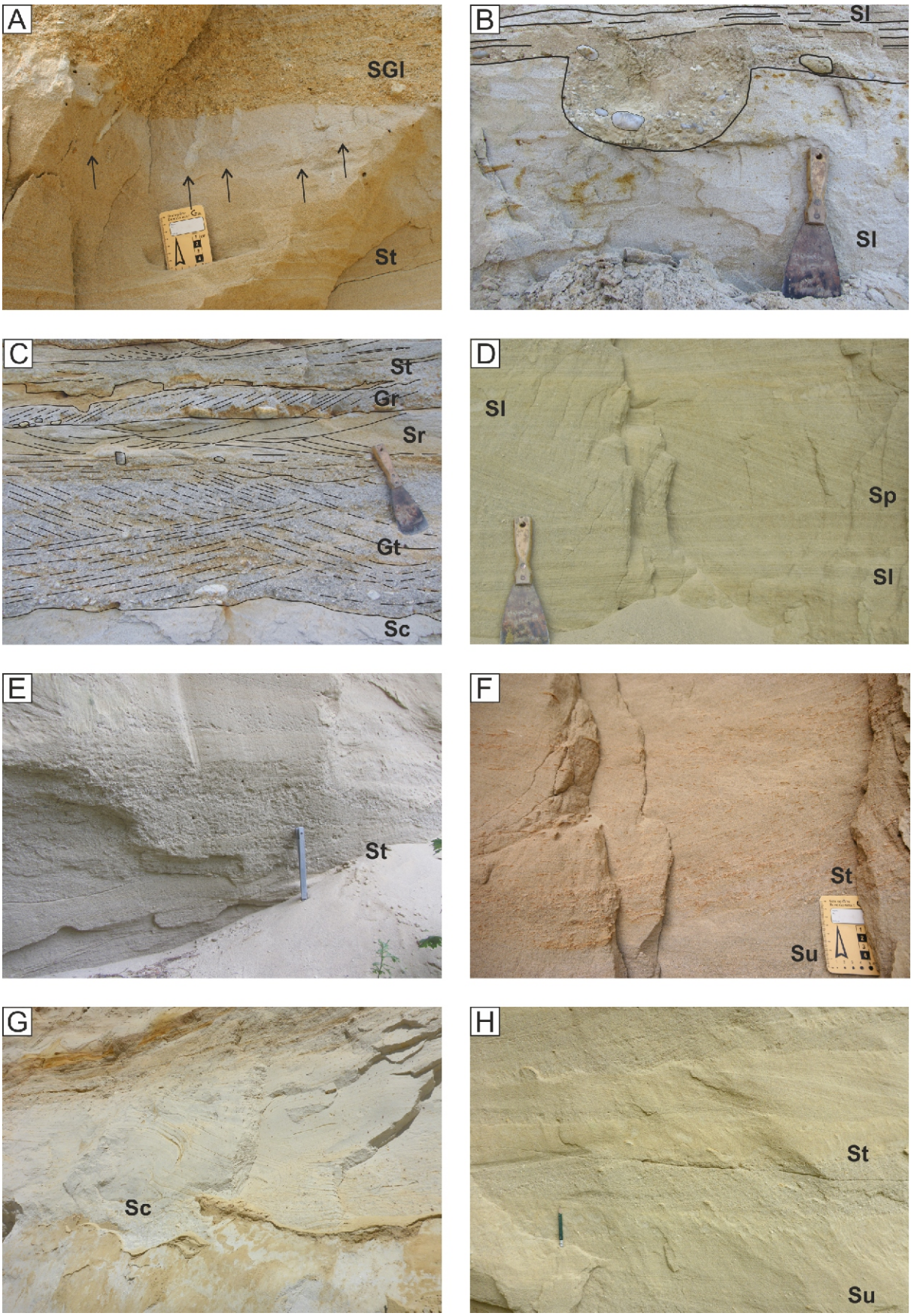

Fig. 6. Photos of lithofacies and facies associations (FAs) within the logged sections

A – contact of lithofacies SGl (FA 2) and St (FA 1) with *Skolithos* ichnofacies; **B** – gutter cast above beds of Sl lithofacies; **C** – lithofacies Sc, Gt, Sr, Gr, and St within FA 1; **D** – lithofacies Sl and Sp – FA 1; **E** – lithofacies St – FA 1; **F** – lithofacies Su and St (variant with bivalves); **G** – lithofacies Sc – FA 1; **H** – lithofacies Su and St (variant without bivalves)

eral fining upwards trend of the beds was observed. Thin sandy interlaminae occur locally, which are usually discontinuous. The predominant gravel layers are of granule up to pebble size and are generally relatively poorly sorted. The adjacent deposits to medium thick beds of facies Gr are significantly finer-grained sands (facies Sc, Sr). The Gr-beds are ~15 cm-thick.

An isolated gutter cast was noted along the base of the sand beds (Fig. 6B). It has an almost symmetrical cross-section with steep walls and a rounded base. It is filled with poorly sorted pebbly sand with a clear fining upwards trend. The coarsest pebbles are concentrated along the base.

Interpretation. FA 1 shows a wide range of depositional and erosional processes active on the upper shoreface. The predominant cross-stratified beds (St, Sp) were formed by the migration of nearshore dunes under the influence of asymmetrical wave action or wave action with superimposed unidirectional currents on a wave-dominated upper shoreface (Hartley and Jolley, 1999). Clifton (2006) located decimetre-high lunate megaripples in the area of most intense wave buildup just seawards of the surf zone. The planar cross-stratification with a wide range of individual set thickness represents 2D dunes and the trough cross-stratification 3D dunes. A relatively large coset thickness indicates relatively high dunes (Wignall et al., 1996). Episodic migration of 2D and 3D dunes alternated with erosion and reworking as recorded by internal truncation surfaces (Hartley and Jolley, 1999), indicates a nearshore trough and ridge morphology. Major phases of erosion are connected with bases of St or Sp cosets (Wignall et al., 1996). Nearshore dunes and bars typically develop on gently dipping shorelines, which are usually sand-dominated (Clifton, 2006). The lateral transition of subhorizontal laminae (Sl) into inclined foresets (Sp, St) reflects progradation and aggradation of these dunes, with the parallel laminae representing their surface and the cross-stratification their slopes. The alternation of individual sets of cross-strata and parallel-laminated beds suggest that the set-bounding surfaces are subparallel to the bar surface (Hartley and Jolley, 1999). The absence of any clayey material, the extensive lack of bioturbation or its sparse and local occurrence, and the frequent reactivation surfaces, indicate that the dunes migrated rapidly. The presence of open, disarticulated bivalve shells oriented parallel to the stratification, with predominantly stable/upward-convex positions, suggests redeposition of the bivalves (previously exhumed?) into the shoreface depositional environment (DeCelles, 1987). The apparently uniform taxonomic composition of the bivalves may signal that they originated from mussel banks (Wignall et al., 1996). Transition from shell-less to shell-rich sands of lithofacies Sr and Sp within the succession and sudden and rapid occurrence of shells are interpreted as erosion of a protected backshore area (lagoon?) and a general shallowing-upwards trend.

Facies Su is interpreted as the result of a scour-and-fill process by wave action combined with unidirectional currents and is explained as swaley cross-stratification. Broad, convex-down surfaces, typical of sets of lithofacies Su, are indications of considerable erosion associated with storm events. Sedimentary accretion follows scouring of the wave bottom at a low rate (Dumas and Arnott, 2006). It is supposed that the swaley cross-stratification forms on the shoreface between the fair-weather and storm wave bases. Layers with swaley cross-stratification are commonly accompanied by beds of facies St, Sp or Sl (Fig. 6H). These features testify to considerable variations in flow conditions, from wave oscillation to unidirectional or combined-flow (Massari and Parea, 1988).

Lenses of fine to medium sand of the bioturbated facies Sb are rare, isolated, and spatially restricted. Low bioturbation intensity and low trace fossil diversity are interpreted as the result of rapid deposition and episodic biogenic activity. The S*kolithos* ichnofacies is typical of sandy shores. The rare and restricted occurrence of facies Sb within the sands of facies Sr and Sl of similar grain size corroborates the shoreface depositional environment.

Beds of facies Gr are interpreted as evidence of storm-wave driven gravelly megaripples (Leckie, 1987; DeCelles, 1987; Hart and Plint, 1995) based on their preserved forms. The nearly symmetrical convex-up morphology indicates deposition and reworking by oscillatory flows, i.e., the action of waves. Gravelly megaripples form under oscillatory and/or combined flows in coarse to pebbly sands under the same hydraulic conditions as hummocky cross-stratification in fine sands. The characteristic textural bimodality is an effect of post-storm wave-orbital currents which winnowed away finer-grained material and the rhythmic alternation of coarser beds and finer interbeds suggests that each gravel/sand couplet represents the record of storm and subsequent recovery stages (DeCelles, 1987; Massari and Parea, 1988). Gravelly megaripples are typically reported from gravelly shorelines (Hart and Plint, 1989, 1995) where they develop as elongated linear stripes trending at a high angle to the palaeoshoreline.

Gutter casts are “downward-bulging erosional structures” that may be isolated from or amalgamated to the bases of sandstone beds (Whitaker, 1973; Myrow, 1992; Collins et al., 2017). The lack of loading, dewatering and soft-sediment deformation and the fining upwards trend in gutter cast infills indicate a close linkage between processes controlling both the initial erosion of the substrate and subsequent rapid deposition (Collins et al., 2017). The surface geometry is entirely erosional. Very steep scour walls that are steeper than the angle of repose of the sand-sized wall material indicate rapid aggradation. Gutter cast erosion is generally ascribed to powerful unidirectional currents generated during the rising and peak phase of storm (Myrow, 1992; Collins et al., 2017). They form when large waves drag gravel back and forth on a sandy bed during a storm (Clifton, 2006). According to Lamb et al. (2008) or Collins et al. (2017) gutter erosion and infill likely occur under oscillatory-dominant or purely oscillatory flow generated by shallow-marine storms. A general shoreline-normal orientation is typical of most gutter casts (Myrow and Southard, 1996).

Penecontemporaneous deformation (lithofacies Sc) which imply syn- or early post-depositional liquefaction and/or fluidization only locally affects one of the dominant lithofacies, Sl. They may provide evidence of rapid sand deposition and/or wave impact on the bottom during high-energy events (Massari and Parea, 1988). However, the close proximity of the Sc bed to a fault may link the bed to local synsedimentary tectonic activity (cf. Fig. 2).

Palaeocurrent analysis based mostly on orientation of the cross-stratified beds (n = 23) clearly reveals a transport direction mostly towards the SW, less commonly to the WSW, S, SE or ESE (i.e., seawards). A transport direction towards the NE (i.e., coastward) was the exception (compare Fig. 14A in Discussion).

FA 2 – FORESHORE DEPOSITS

This facies association is subdivided into two sub-associations based on textural characteristics. These sub-associations were identified in different parts of the sand pit, i.e., they are spatially/laterally separated. The more common and thicker sub-association FA 2a is composed by lithofacies SGl and Gm. The thickness of the tabular beds of FA 2a varies between 0.35 and 1.5 m. FA 2a erosively cuts the underlying FA 1 and is overlain by FA 1. The rare finer-grained sub-association FA 2b is composed of lithofacies Sl and Sr. The layer of FA 2b is tabular and only 0.2 m thick. FA 2b overlies FA 1 and is overlain by FA 4.

While lithofacies SGl strongly dominates in FA 2a, lithofacies Gm is only observed in the basal part of the succession, where it drapes a slightly irregular erosional surface with low local relief as a thin layer of mostly pebble-, or rarely cobble-gravel. The erosional surface generally truncates fine-grained, well-sorted sands (lithofacies Su or St) commonly with scattered subvertical burrows and a bioturbation index BI (*sensu* Droser and Bottjer, 1986) of 0 to 1 (Fig. 6A). The thickness of the Gm layer varies from one pebble up to 15 cm. Pebbles and rare cobbles are usually well-rounded to rounded and formed from stable rocks (kaolinised granitoids or quartz). The long axes of pebbles or cobbles are usually oriented parallel to the bedding and/or bounding surface. The layer of lithofacies Gm is traceable laterally along the entire exposed sand pit wall. Facies SGl is formed by poorly sorted coarse- to very coarse-grained sands with scattered granules and pebbles. Gravel clasts are angular to subangular, subrounded or rounded and their long axis is usually oriented parallel to the stratification. The subparallel planar stratification is locally slightly uneven/undulose and either horizontal or inclined at a low angle (~5°). The medium thick beds of facies SGl have roughly horizontal bases and flat tops. While the tops are sharp, the deposits at the bases gradually pass from facies Gm. Trace fossils are missing.

Sub-association FA 2b is dominated by medium- to coarse-grained sands of facies Sl with low-angle planar stratification. Usually thin and tabular beds are slightly bioturbated (*Skolithos* ichnofacies). Thin beds of fine sand of facies Sr overlie facies Sl and reveal ripple cross-lamination. Ripple forms are asymmetrical with sigmoidal foreset laminae.

Interpretation. Facies Gm is interpreted as a layer produced by the winnowing action of surf-zone waves (DeCelles, 1987). The lag is derived from the reworking of the crystalline basement/substrate (Massari and Parea, 1988; Hartley and Jolley, 1999). Multiple reworking resulted in the mineralogical and textural maturity of the pebbles. Facies Sl and SGl are interpreted as the result of swash and backwash processes on the foreshore, and facies Sr similarly reflects the action of waves and wave-induced currents in a lower flow regime. The beds of FA 2 appear to have been deposited on the foreshore, while FA 2a represents a foreshore with a significant supply of gravel clasts, FA 2b was deposited on a more "protected" sandy foreshore.

FA 3 – GRAVELLY BEACH DEPOSITS

The facies association FA 3 consists of stratified, sheetlike beds of pebble-cobble gravel. Dominantly rounded clasts of gravels look mostly fresh, but some more intensely weathered pebbles/cobbles were also recognised. Clast size varies from pebbles to boulders. Clast surfaces lack encrusting organisms. Beds of FA 3 have a tabular shape and they were formed in very close proximity to the granite bedrock as shown by geological mapping. Although no direct contact was available for documentation, the bedrock is exposed at several locations on the pit floor just a few metres laterally from the documented logs. The towering granite ridges and swells are rounded and partially smoothly polished (Fig. 7A).

The deposits of FA 3 also overlie the beds of FA 1. The thickness of FA 3 beds varies between 1.0 and 2.0 m in the exposures studied; however, it is only of minimal thickness because the upper surface of FA 3 coincides with the present land surface and is influenced by landscape morphology.

FA 3 consists of three facies, Gg, Gb, and Gi, with facies Gg being the most common. The openwork to clast-supported cobble to pebble gravel of lithofacies Gg is massive, coarse tail normal graded, without any evident preferred orientation of clasts or clast shape separation (Fig. 7E). An enrichment of large cobbles along the base of the beds is typical. Facies Gb was recognised above facies Gg. Cobble gravel of lithofacies Gb is enriched in large cobbles and boulders, massive, clast-supported to openwork with open spaces filled with pebbles or coarse sand (Fig. 7B, F). Pebble shape segregation and imbrication are absent. Pebble to cobble gravel of facies Gi typically consists of large pebbles and cobbles aligned parallel to the bases of beds and have a clast-supported to openwork texture. Imbrication (n = 15) is mostly towards WNW, SW (seaward-dipping), less commonly towards NE (coastward) was documented (see Fig. 5). The bed of facies Gi is sandwiched between beds of facies Gg. At some locations, sheets of lithofacies Gg are overlain by lithofacies Gb, while in other locations almost exclusively stacked sheets of lithofacies Gg (with thin interbeds of Gi) form amalgamated or multistorey bodies.

Interpretation. FA 3 is interpreted as tabular gravel bodies of the foreshore/gravel beach in a high-energy setting (Nemec and Steel, 1984; Watkins, 1992). Facies Gb represents a low-maturity clast assemblage (*sensu* Bluck, 1999) with a relatively minor role of shape sorting. The size-sorting is documented only by the removal of sand and granules and the formation of a gravel framework. This indicates a wave and current activity. The framework of boulders and cobbles is filled and also followed by finer-grained material, suggesting deposition in the subaqueous zone of a beach, possibly in the outer frame zone (Bluck, 1967; Postma and Nemec, 1990). However, a crown of coarse clasts was also identified along the highest (i.e. also the most landward) part of gravelly cusps or berms (Bluck, 2011).

Facies Gg represents a moderately mature clast assemblage (*sensu* Bluck, 1999). Although the importance of shape sorting in the clast assemblage is still low, size-sorting is documented not only in the removal of sand and granules and the formation of a gravel framework but also in the strong reduction of boulders. This points to a prolonged importance of wave and current activity along the beachface. Deposition in the subaqueous zone of a beach, probably in the infill zone, is inferred (Postma and Nemec, 1990; Bluck, 1999). Normal grading could have developed due to wave reworking by mobilizing and redepositing the upper part of a tabular gravel sheet during a storm event (Evans and Holm-Denoma, 2018).

Facies Gi represents the clast assemblage of the highest recorded maturity (*sensu* Bluck, 1999). Size-sorting is documented by the progressive removal of the finest and the coarsest clast sizes, as well as the role of shape sorting (a relatively increased number of discs and reduction of spheres) and preferred orientation. This suggests a greater role of wave and current activity typical of the higher subaqueous zone of a beach. Since the disc-shaped clasts are not predominant in the pebble shape spectra, the facies is interpreted as the imbricate-disc zone to infill zone (Bluck, 1967; Postma and Nemec, 1990), i.e., the foreshore environment.

The recurring motif of undulose surfaces covered by outsized cobbles to boulders, with alternations of relatively coarser and finer layers and clast-supported to openwork framework, is interpreted as accretion of successive gravel sheets and alternations of periods of different wave regime, storm activity and/or variations in clast supply. During a depositional period, gravel sheets were deposited, whereas during a storm period, the coarse material was reworked into a lag and the finer material was eroded. Similarly, Massari and Parea (1988) use the low-angle erosion surfaces as evidence of storm wave planation of the beachface. The horizontal or low-angle beds of facies Gg, Gi and Gb are interpreted as selection pavements

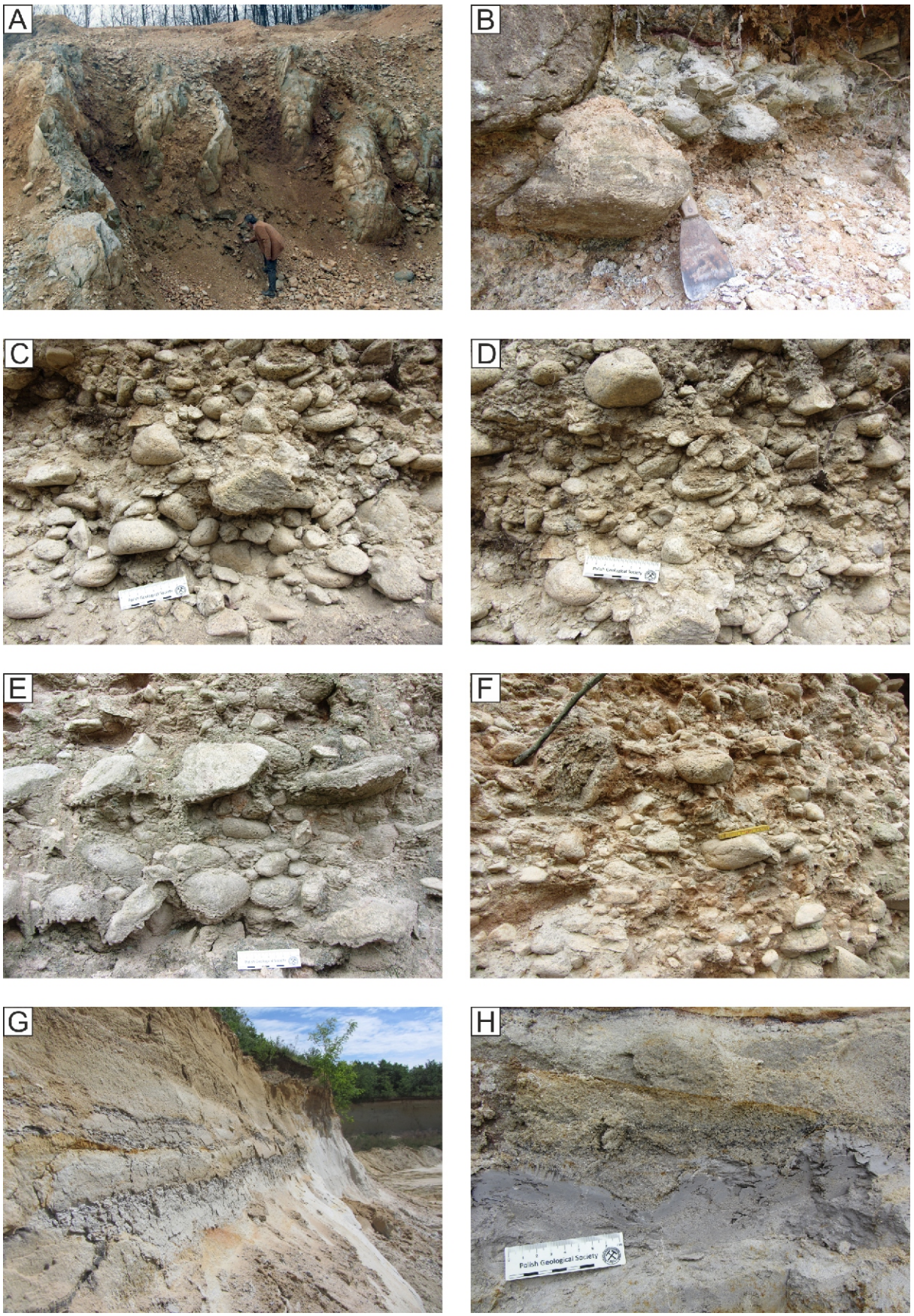

Fig. 7. Photos of lithofacies and facies associations (FAs) within the logged sections

A – gravel pit at Rosenau "Pfarrgrube", gravel-filled pockets between granite ridges; **B** – clast shadow within lithofacies Gb (FA 3); **C** – openwork texture; **D** – lithofacies Gi; **E** – lithofacies Gg; **F** – fresh *versus* intensely weathered pebbles/cobbles of granites of the Thaya Batholith – lithofacies Gg; **G** – NE wall of the Diem sand pit with occurrence of FA 3; **H** – erosive top of lithofacies Fl (FA 3)

and the beds with more steeply inclined and undulose bases and tops as cusps and berms (Bluck, 1999). Similarly, Maejima (1982) interpreted broad, concave-up scour surfaces as the effect of cusp formation. A general increase in the inclination of gravel beds in the exposures might reflect progradation of the stacked beachface (gravelly foreshore).

The absence of the large-disc zone and of sand layers within the gravels, a very reduced occurrence of the imbricate zone, and the strongly dominant role of the infill zone are typical features of FA 3. The scarcity of a large-disc zone facies might reflect complete submergence of the beach and erosion of this zone (see Postma and Nemec, 1990). However, although clast shape variations play a crucial role in recognition of the beach zones, the nature of the original rocks, of which the clasts are made, also controls the clast shape distribution, especially in less mature beaches (Bluck, 2011). The granites of the Thaya Batholith are probably more prone to disintegrate into equant/spherical fragments.

FA 4 – BACKSHORE – LAGOONAL DEPOSITS

Deposits of FA 4 are wedge-shaped. The maximum observed thickness of FA 4 was ~1 m. A significant reduction in the thickness of FA 4 and its complete absence in the SE and E parts of the Diem sand pit indicate that FA 4 was preserved only as an erosional relic and its preservation was probably significantly influenced by basement morphology. FA 4 is sandwiched between deposits of FA 2 (see Figs. 4B and 7G), where the fine-grained sub-association FA 2b was recognised below FA 4 and the coarser FA 2a above it.

FA 4 comprises four lithofacies (Sg, Sm, Sl and Fl). Non-channellised and laterally extensive mudstone of facies Fl represents the most characteristic component of this FA. No plant and wood fragments nor other fossils were observed. Medium to thin beds of facies Fl alternate with mostly thin and tabular beds of facies Sg, Sm and Sl. An erosive contact of these sandy facies is typical if they overlie mudstones. Isolated angular intraclasts (up to 3 cm across) of mudstone of facies Fl were observed in the deposits of facies Sg.

Interpretation. The mudstone dominance and the vertical and lateral association with FA 2 indicate deposition in an area protected from wave activity, i.e., in a lagoon/backshore. The absence of plant and wood fragments points to isolation from terrigennous organic input, and together with absence of desiccation cracks, a “stable” subaqueous environment and a reduced freshwater input. Tabular/sheet bodies of massive sand or those with planar, uneven lamination (facies Sg, Sm, Sl), typically normal grading or a fining upwards trend and predominantly thin-bedded sandy facies represent relatively proximal (facies Sg) and distal deposits (Sl, Sm) of a washover fan or fans and indicates transport of coarser marine sediments landwards into the lagoon. Washover fans represent storm-generated sheet-flow deposits that are usually biologically affected during fair-weather periods, especially in their distal parts (Allen and Johnson, 2011). The lack of evidence of such activity points to rapid deposition or hostile conditions. The lack of fossil content within FA 4 is interpreted similarly. The source of the bivalve shells, recognised as open, disarticulated shells in some parts of FA 1, must have been located in a different part of the coastal depositional system than preserved in FA 4.

GRAIN SIZE AND PROVENANCE ANALYSIS

Grain size data mainly characterise the energy of the depositional medium (Reineck and Singh, 1980) and the changes during sedimentation of the different formations and provide comparable mathematical data of mean grain size and sorting.

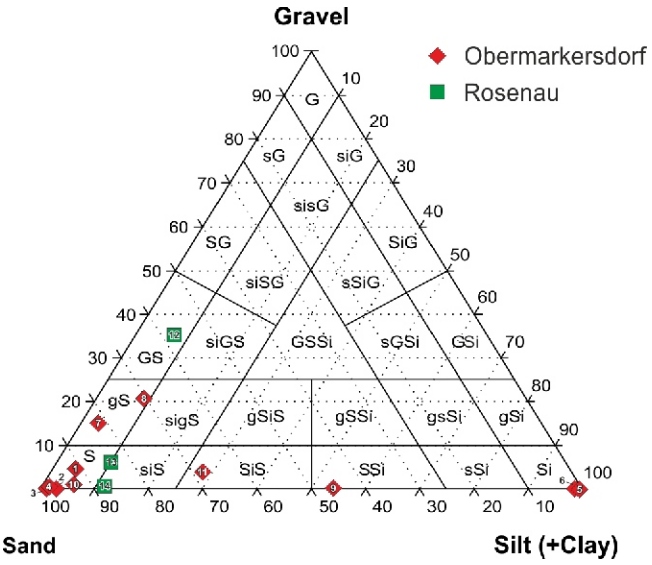

Fig. 8. Results of grain size analysis from the Diem sand pit (Obermarkersdorf) and Rosenau sand and gravel pit in a ternary diagram gravel-sand-silt (+clay)

For grain-size data and position of samples refer to Table 2 and Figures 2, 3, 4B, C

Provenance studies provide data about the source area, which might be especially important in the case of complex geology of the backshore or coastal physiography and provide evidence about possible unpreserved rocks in the source area. Results of provenance analyses are based on a combination of evaluation of pebble petrography and light and heavy mineral studies. Provenance data in combination with palaeocurrrent patterns can constrain the role of onshore-offshore and alongshore transport. For that reason, some provenance data are compared with similar data from the nearby (~14 km SW) locality of Maigen, which is situated SW of the study area in the shallow marine Eggenburg Bay (Nehyba and Roetzel, 2021).

GRAIN SIZE DISTRIBUTION

Grain size data show a clear lithological difference between the basal and the upper part of the Burgschleinitz Formation in the Diem sand pit as well as in the abandoned sand and gravel pit north-west of Rosenau, west of a war memorial (Figs. 2, 4C and 8, Table 2).

In the basal Diem sand pit, except for the coarse-grained intercalations, these are mainly medium- to fine-grained sands with a sand content of 91.2–98.9%. They have very low gravel (0–4.6%) and equally low silt and clay contents (silt: 0.4–2.7%, clay: 0.1–1.5%). This results in an average grain size (mean) of 1.87–2.2 and a standard deviation (sorting) of 0.87–1.74, reflecting moderate to poor sorting (Friedman, 1962). Occasionally, however, slightly siltier deposits (siltsands) occur with ~4% gravel, 68% sand and 28% silt and clay.

In contrast, the deposits from the hanging wall of the Diem profile are usually much coarser. They are gravelly coarse- to medium-grained sands with a gravel content of 15–20.6% in which fine gravel predominates. The sand content between 70.6 and 81.8% is significantly lower and the fine fractions significantly higher than in the basal parts of the profile (silt:

Table 2

Grain size data for the Burgschleinitz Formation in the Diem sand pit (OM) and the Rosenau sand and gravel pit, west of the war memorial (ROS)

No	Sample	Gravel [%]	Sand [%]	Silt [%]	Clay [%]	Mean Mz	Stdev $_I$
1	OM-65	4.6	91.2	2.7	1.5	1.87	1.74
2	OM-65a	0.0	97.1	2.4	0.5	1.99	1.05
3	OM-66	0.0	98.9	0.4	0.7	1.93	1.36
4	OM-67	0.5	98.1	1.3	0.1	2.10	0.87
5	OM-67b	0.0	0.3	76.2	23.5	8.01	2.47
6	OM-67c	0.0	1.2	69.0	29.8	8.29	3.19
7	OM-68	15.0	81.8	2.1	1.1	0.60	1.98
8	OM-69	20.6	70.6	8.5	0.3	0.57	2.10
9	OM-N-1	0.0	53.2	46.8		4.10	2.60
10	OM-N-2	0.4	95.9	3.7		2.20	0.90
11	OM-N-3	4.0	67.9	28.1		4.80	1.40
12	ROS-1	35.1	57.7	2.7	4.5	0.35	3.20
13	ROS-2	0.6	87.9	7.0	4.6	2.44	2.82
14	ROS-3	6.1	84.0	5.3	4.7	1.38	3.07

The average grain size (Mean) is expressed by the first standardised moment (Mz), the uniformity of the grain size distribution/sorting by the second standardised moment (graphic standard deviation Stdev $_I$); Number (No) refers to sample points in Figures 2, 3 and 4B, C

2.1–8.5%, clay: 0.3–1.1%). The average grain size (mean) of the deposits is therefore significantly lower (0.57–0.6) and values of 1.98–2.1 of the standard deviation (sorting) indicate poor to very poor sorting. Similar grain size distributions were also found in the Rosenau sand and gravel pit, west of the war memorial (Figs. 3 and 8, Table 2).

The pelitic intercalations in the basal part of the Diem sand pit (Fig. 2, section 1 and 3; Figs. 4B and 8) are clayey silts and claysilts dominated by 69–76.2% silt and 23.5–29.8% clay. Values of mean grain size are therefore quite high (8.01–8.29) and the standard deviation (sorting) of 2.47–3.19 corresponds to very poor sorting. Even in sandier parts of this section with sandsilts, the pelitic content can be close to 50%.

PETROGRAPHY AND SIZE OF CLASTS

The gravels of FA 3 are classified as monomict when only granite forms pebbles, cobbles and boulders. However, several varieties of granite could be recognised with differences in the grain size (fine-grained vs. more porphyritic varieties) and intensity of weathering. Although relatively “fresh” clasts strongly dominate, more strongly weathered cobbles and pebbles were also observed (see Fig. 7F). The largest recognised boulder was ~90 cm across, while cobbles and pebbles strongly dominate in the clast spectra.

The petrography of the coarsest (gravelly) portion of the sands of FA 2 and FA 1 differs slightly, and these deposits can be classified as polymict. Granite pebbles play an important role and form 30–54.4% of pebble spectra. Kaolinised feldspars are frequent. These pebbles are mostly of spherical shape, followed by blades and rods. Discs are less common. Subrounded clasts strongly dominate (68.9–80%), followed by rounded ones. Subangular clasts form ~10% of the spectra. Quartz-feldspar aggregates (16–30.8%) are also present, originating from granites of the Thaya Batholith (grus), and have the same distribution of the clast shape and rounding as observed in the granite clasts. These pebbles are mostly of spherical shape, followed by blades. Rods and discs are less common. Subrounded clasts strongly dominate (67.6–78.6%), followed by rounded ones. Subangular clasts form ~10% of the spectra.

Some of the samples studied show an increased content of quartz pebbles, between 13.5 and 43.3%. Subrounded pebbles predominate (77–77.8 %); subangular pebbles are less common (20.3–29.7%). Angular or well-rounded quartz pebbles are very rare. Spherical quartz pebbles strongly dominate (73.7–85.9%). Other shapes (blade, rod, disc) form only a few percent. Pebbles from metamorphic rocks (quartzite, mica schist) are the least common among the rock pebbles, reaching 0.5–10%. These pebbles are mostly subangular, and rarely angular or subrounded. They are mostly bladed or rod-shaped.

PETROGRAPHY OF LIGHT MINERALS

The sands of FA 1 and 2 can be classified in equal proportions as lithic arenites (50%) and arkosic arenites (50%; *sensu* Pettijohn et al., 1987). The classification diagram of Folk (1968) or Okada (1971) for the samples studied is shown in Figure 9A. The samples studied are mineralogically immature.

In the basal part of the Diem sand pit, the quartz content is 53–57%, the feldspar content 22–29% (alkali feldspar: 5–9%, plagioclase: 12–22%) and the proportion of lithic components (rock fragments, polycrystalline quartz, mica) 17–25%. In contrast, in the hanging wall of the profile, the quartz content (40–48%) decreases, while the lithic components (28–35%) increase. The plagioclase content is also here always significantly higher (18–22%) than the proportion of potassium feldspar (2–7%).

The average content of quartz is 51.8%, while feldspar forms 23.7% and lithic fragments 24.6%. Plagioclase (AVG 17.5%) always dominates over alkali feldspar (6.2%), as also seen in the QPK diagram (Fig. 9B; Girty et al., 2003). Compared to the samples from the Maigen area in the Eggenburg Bay (Nehyba and Roetzel, 2021), the plagioclase content of the samples from the Obermarkersdorf area is significantly higher. Together with the higher quartz/feldspar ratio this indicates the important role of a first-cycle source in the samples from the Diem sand pit, while a greater role of recycling and weathering is evident in the samples from the Maigen area (Nehyba and Roetzel, 2021).

In the QFL discrimination diagram (Fig. 9C), both the samples from the Diem sand pit and from the Maigen area occupy the recycled orogenic field related to a continental/craton source. Such a distribution reflects the different sources of the most cratonward part of the distal Alpine-Carpathian Foredeep Basin, where the material from crystalline metamorphic rocks is mixed with that from granitoids. Although the samples from the Obermarkersdorf and Maigen area (Nehyba and Roetzel, 2021) reveal a generally common origin, some differences in provenance are evident. The sands from the Maigen locality range from sublithic to lithic arenites, indicating a higher proportion of supracrustal rocks (sedimentary+metamorphic rocks). In the sands from the Diem sand pit, on the other hand, the proportion of plutonic rocks is relatively higher.

HEAVY MINERALS

Heavy minerals are sensitive indicators of provenance, weathering, transport, deposition and diagenesis (Morton and Hallsworth, 1994). Heavy mineral assemblages, ratios of ATi (100 x apatite count/total apatite plus tourmaline), GZi (100 x garnet count/total garnet plus zircon), RuZi (100 x rutile count/total rutile plus zircon), GTi (100 x garnet count/total garnet plus tourmaline; Morton and Hallsworth, 1999) and the ZTR index (total zircon plus tourmaline plus rutile) were evaluated. The mineral ratios GTi, GZi, ATi, and RuZi (according to Morton and Hallsworth, 1994) were used as good indicators of source rock characteristics (since they are comparatively immune to alteration during the sedimentary cycle), to indicate successive stages in provenance evolution and tectonic history, and as indicators of sediment transport paths. The ZTR index is widely accepted as a criterion for the mineralogical "maturity "of heavy mineral assemblages (Hubert, 1962; Morton and Hallsworth, 1994) in the case of derivation from a similar source. The proportion of opaque versus translucent minerals (OP/TR) was counted to provide further information on weathering and reworking conditions.

The heavy mineral assemblages (cf. Roetzel and Kurzweil, 1986; Roetzel and Heinrich, 1999) reveal remarkable differences between the localities studied (see Table 3A). Whereas the heavy mineral assemblage of the Obermarkersdorf locality

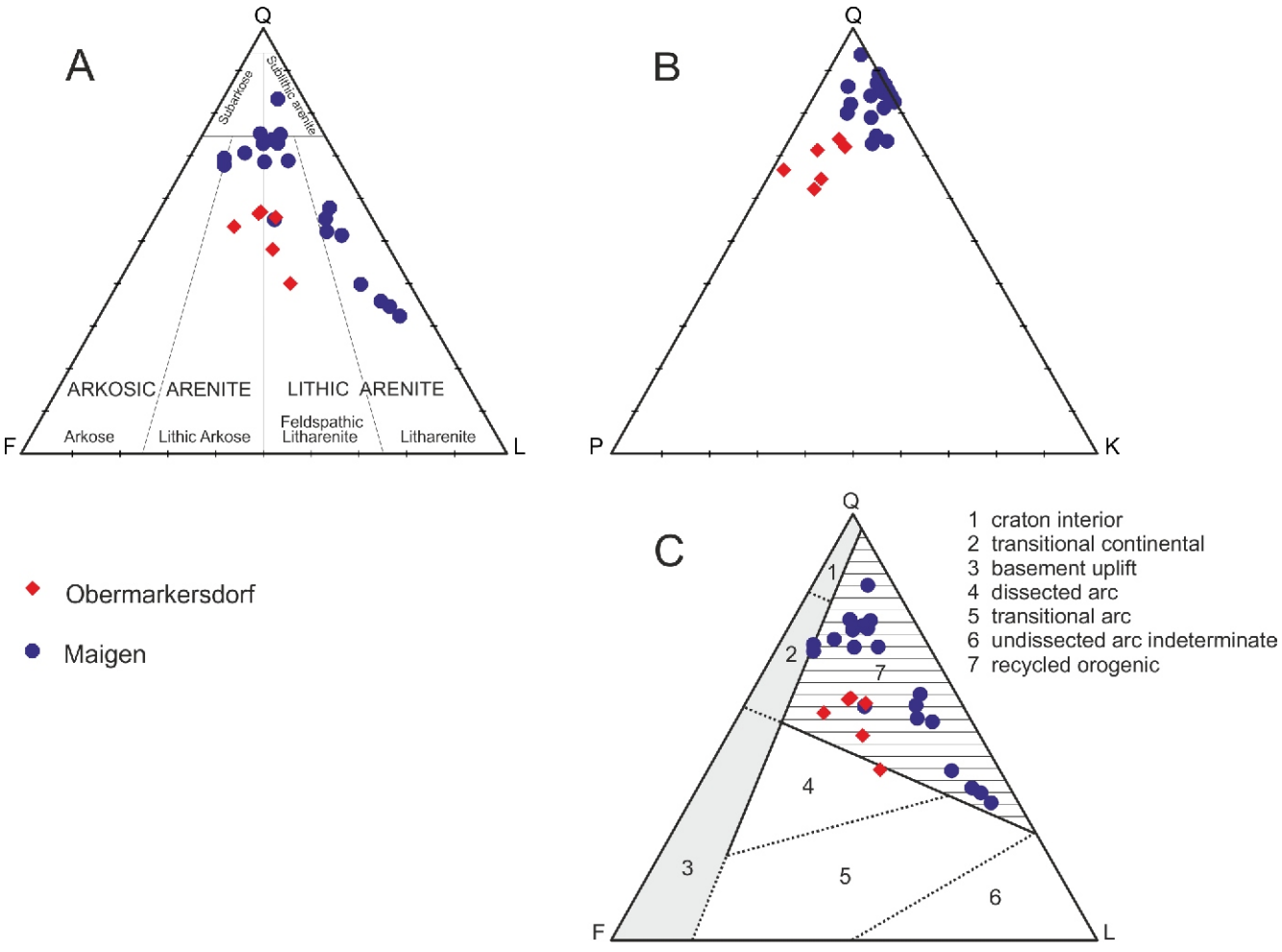

Fig. 9. Discrimination ternary diagrams of petrography of light minerals for samples from the Diem sand pit (Obermarkersdorf) in comparison with samples from Maigen (Nehyba and Roetzel, 2021)

A – QFL classification diagram after Folk (1968) and Okada (1971) for the samples studied; **B** – QPK diagram (Girty et al., 2003) for the samples studied; **C** – QFL discrimination diagram for the samples studied (Dickinson, 1985); Q – total quartz, F – total feldspar (plagioclase + alkali feldspar), P – plagioclase, K – alkali feldspar, L – total lithic components

Table 3A

Heavy mineral data (median) of the Burgschleinitz Formation at individual localities (Obermarkersdorf, Rosenau, Maigen)

Heavy mineral	Obermarkersdorf Median % (Min.–Max.)		Rosenau Median % (Min.–Max.)		Maigen Median % (Min.–Max.)	
Zircon	2.4	(0–3.6)	9.8	(3–13.3)	6.6	(0–17)
Rutile	2.6	(0.5–2.9)	1.3	(0–2.6)	10.6	(0–17)
Titanite	0.5	(0–1)	–		0.4	(0–2)
Tourmaline	11.5	(6.6–17.8)	2.6	(0–6)	23.5	(7–38)
Garnet	8.4	(5.6–10.6)	33.8	(15.8–55.7)	4.2	(0–18)
Staurolite	39.0	(31.2–42.8)	3.2	(0.9–7.4)	26.72	(6–70)
Kyanite	8.4	(6.7–12.1)	1.6	(0.7–2.5)	16.0	(2–29)
Sillimanite	3.7	(2.4–5)	0.3	(0–1)	8.5	(0–22)
Andalusite	3.5	(2–5)	–		1.9	(0–7)
Apatite	0.5	(0–1)	0.2	(0–0.5)	0.1	(0–1)
Epidote+Zoisite	16.2	(7.7–20.9)	44.2	(19.1–67.3)	1.1	(0–3)

Table 3B

Values of heavy mineral data of ZTR (total zircon plus tourmaline plus rutile), ATi (100 x apatite count/total apatite plus tourmaline), GZi (100 x garnet count/total garnet plus zircon), RuZi (100 x rutile count/total rutile plus zircon), and OP/TR (proportion of opaque *versus* translucent minerals) for localities of the Burgschleinitz Formation

Heavy mineral ratio	Obermarkersdorf Median % (Min.–Max.)		Rosenau Median % (Min.–Max.)		Maigen Median % (Min.–Max.)	
ZTR	15.7	11.8–24	13.7	3–19.9	48.87	8–56
ATi	3.9	0–6.6	33.3	0–100	0.5	0–6.7
GZi	77.9	60.8–100	78.1	70.2–84.4	39.3	0–100
RuZi	58.7	41.9–100	8.4	0–15.8	62.7	33.3–100
OP/TR	0.4	0.3–0.5	0.9	0.2–1.5	1.1	0.3–4.9

(Diem sand pit) can be described as a staurolite-epidote-zoisite-tourmaline assemblage, the assemblage for the locality Rosenau reveals a high content of zoisite-epidote and garnet. The values of ZTR, GTi, RuZi, ATi, and OP/TR ratios are shown in Table 3B. Although the ZTR values are similar, the role of individual minerals varies. Whereas tourmaline dominates in the Obermarkersdorf exposure, zircon is the most important "superstable" mineral at Rosenau. The varied role of tourmaline and zircon are also reflected in highly varied ATi and RuZi ratios for these two localities.

The results show variable amounts of opaque, stable (staurolite, garnet, apatite, and titanite) and moderately stable (epidote, sillimanite, kyanite, and andalusite) minerals. The content of ultrastable minerals (zircon, tourmaline, and rutile) is relatively low and unstable minerals (hornblende, pyroxene, sphene, and spinel) were extremely rare.

Despite the vicinity to the granite of the Thaya Batholith, the spectra of transparent heavy minerals are characterised by staurolite, epidote-zoisite and tourmaline along with garnet, kyanite and sillimanite. Tourmaline is present in larger quantities especially in the basal parts of the profile, while epidote-zoisite and to a slight degree also garnet increases towards the top. The ternary diagrams of the heavy minerals are shown in Figure 10. The dominance of different ultrastable minerals for individual localities is evident.

GARNET COMPOSITION

Detrital garnet chemistry is often used for more precise identification of source rocks (Morton and Hallsworth, 1994). Eight garnet types were identified in the deposits of the Burgschleinitz Formation studied (see Table 4).

Multivariate analysis of garnet chemistry, according to Tolosana-Delgado et al. (2018), revealed four sources of garnet. The predominant source was amphibolite facies metamorphic rocks (64.73%). Less common were garnets from granulite facies metamorphic rocks (14.7%) or garnets from eclogite facies metamorphic rocks (8.7%). Garnets from igneous rocks (11.8%) were also partly involved.

Several ternary discrimination plots were used for more detailed identification of the primary garnet source (Fig. 11). The PRP-ALM+SPS-GRS diagram (Mange and Morton, 2007) in Figure 11A reflects the predominant source of garnets from metasomatic rocks, and very low-grade metamafic rocks

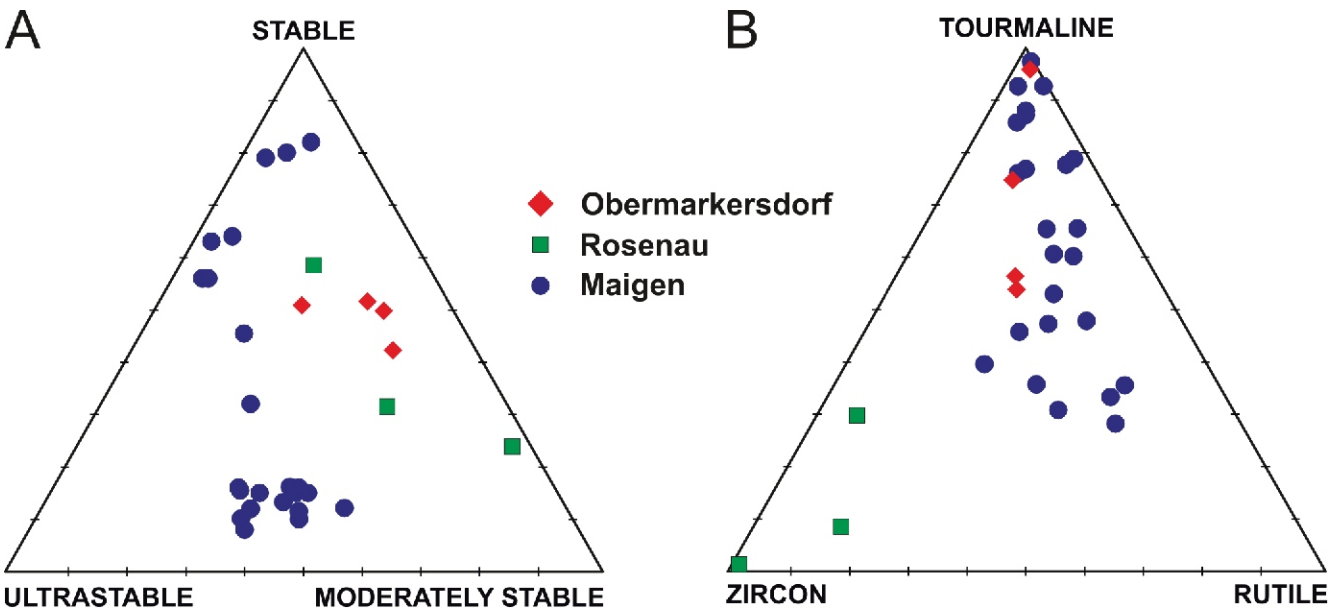

Fig. 10. Heavy mineral ternary diagrams for samples from the Diem sand pit (Obermarkersdorf) and Rosenau sand and gravel pit in comparison with samples from Maigen (Nehyba and Roetzel, 2021)

A – ternary diagram of stable (staurolite, garnet, apatite, titanite) – moderately stable (epidote, sillimanite, kyanite, andalusite) – ultrastable (zircon, tourmaline, rutile) heavy minerals; **B** – ternary diagram of the ultrastable heavy minerals zircon, tourmaline and rutile

(65.7%). Significantly less common are garnets from ultramafic rocks such as pyroxenites and peridotites or from intermediate to felsic igneous rocks (8.6% each). Even rarer were sources from amphibolite-facies metasedimentary rocks (5.7%) or from high-grade granulite-facies metasedimentary and intermediate felsitic igneous rocks (2.9%).

The PRP-ALM-GRS diagram (Aubrecht et al., 2009) in Figure 11B shows that most (62.9%) of the garnets are from broad spectra of rocks such as blueschists, skarns, serpentinites and igneous rocks. Garnets from eclogite- and granulite-facies rocks are less common (22.9%). Garnets from gneisses and amphibolites metamorphosed under amphibolite-facies conditions are rare (11.9%). Garnets from high- to ultrahigh-pressure metamorphic rocks such as eclogites and garnet peridotites are very rare (2.9%).

The diagram GRS-SPS-PRP (Fig. 11C) enables a comparison to some potential source rocks on the eastern margin of the Bohemian Massif (Otava et al., 2000; Čopjaková et al., 2002). A significant part of the garnets might originate from the Moravian Unit (74.3%).

Table 4

Recognised garnet types in the deposits of the Burgschleinitz Formation

Garnet type	
$GRS_{69-86}ALM_{13-31}SPS_{0-1}PRP_{0-3}$	60%
$ALM_{45-54}\ SPS_{39-47}\ GRS_{1-9}\ PRP_{2-5}\ ADR_{1-2}$	8.6%
$ALM_{39-47}PRP_{30-38}GRS_{16-27}\ ADR_{1-2}SPS_{1}$	8.6%
$PRP_{43-49}ALM_{36-40}GRS_{11-18}SPS_{1}ADR_{2-3}UVA_{0-1}$	8.6%
$ALM_{47-49}\ SPS_{24-34}\ GRS_{14-22}PRP_{2-4}\ ADR_{1-2}$	5.7%
$ALM_{63}PRP_{26}GRS_{8}SPS_{1}ADR_{2}$	2.9%
$SPS_{41}ALM_{39}\ PRP_{16}GRS_{3}SPS_{1}$	2.9%
$PRP_{(58)}$-$ALM_{(36)}$	2.9%

COMPOSITION OF RUTILE

Rutile as an ultrastable mineral is commonly used for provenance studies (Force, 1980; Zack et al., 2004a, b; Triebold et al., 2007).

The concentrations of the main diagnostic elements (Fe, Nb, Cr, and Zr) vary considerably in the samples studied. The Fe content shows that 12.5% of the rutiles studied are from magmatic rocks (pegmatites) and 87.5% from metamorphic rocks.

The concentration of Nb ranges from 150 to 16250 ppm (average/AVG 6007.5 ppm), that of Cr varies from 50 to 3900 ppm (AVG 940 ppm), that of Zr ranges from 0 to 1870 ppm (AVG 303 ppm), and most (87.5%) of the logCr/Nb values are negative. Figure 12 shows a discrimination plot of Cr vs. Nb and reveals that the metamorphic rutiles studied originate from metapelites (mica schists, paragneisses, felsitic granulites). According to the diagnostic criteria of Triebold et al. (2007, 2012), all metamorphic rutiles are derived from metapelites. The results of Zr-in-rutile thermometry on metapelitic rutiles (Zack et al., 2004a, b; Meinhold et al., 2008) indicate a broad spectrum of metamorphic rocks (greenschists, amphibolite-facies, eclogite-facies).

ZIRCON STUDIES

Zircon as a very stable mineral is used to evaluate the source rock, the role of recycling and the erosion rate (Poldervaart, 1950; Mader, 1980; Winter, 1981; Lihou and Mange-Rajetzky, 1996). The results of the study are shown in Figure 13.

Euhedral zircons account for 18.1%, subhedral zircons form 31.1%, rounded to subrounded 57.7%, well-rounded 4.7%, and anhedral 6.5% of the zircon spectra. Crystal faces were identified in 44.5% of the zircon grains. Fracturing of zircon grains was relatively common (46.7% of the grain spectra). Grains fractured nearly parallel to the c-axis were significantly more common (44.7%) than grains fractured perpendicular to the

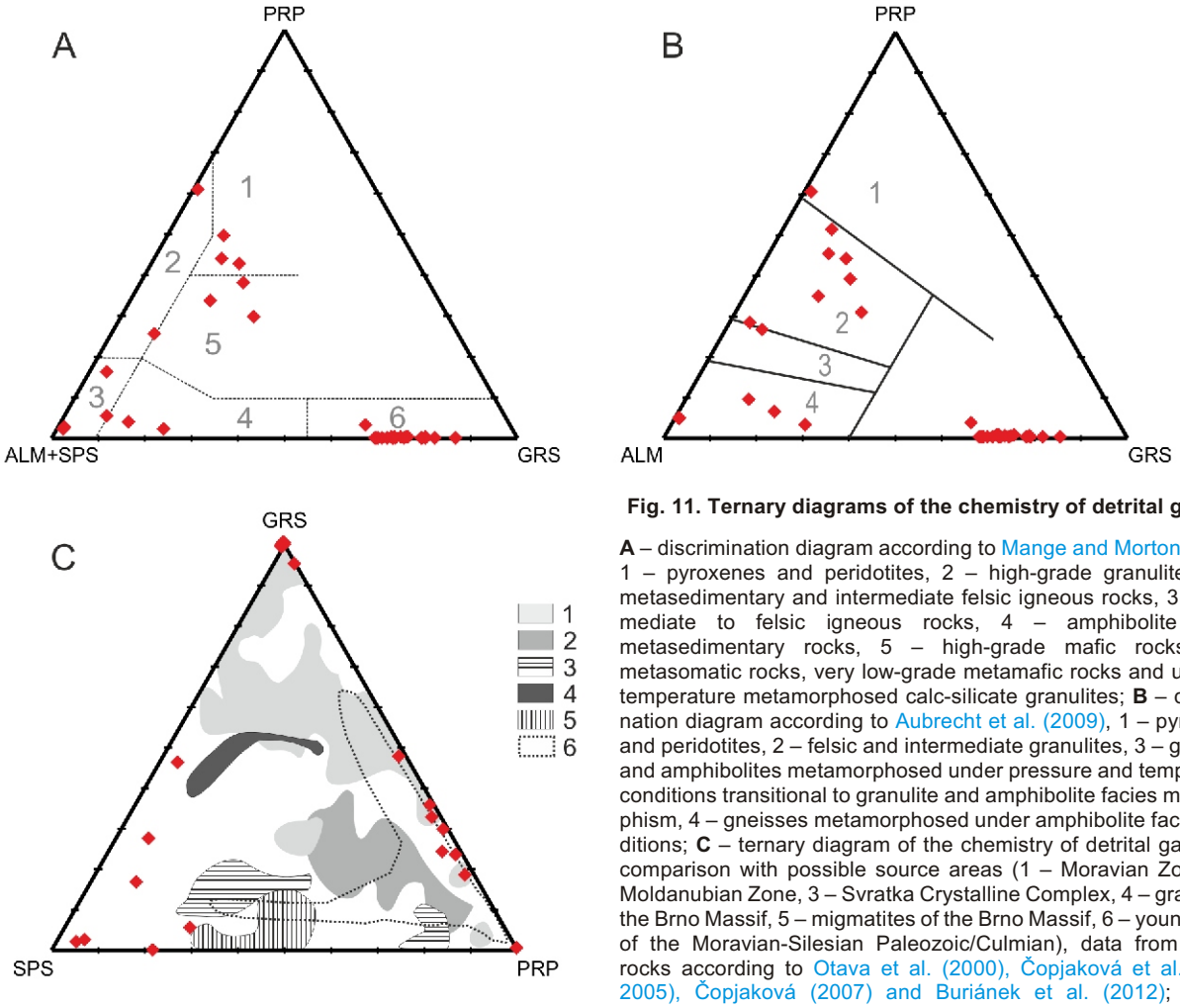

Fig. 11. Ternary diagrams of the chemistry of detrital garnets

A – discrimination diagram according to Mange and Morton (2007), 1 – pyroxenes and peridotites, 2 – high-grade granulite facies metasedimentary and intermediate felsic igneous rocks, 3 – intermediate to felsic igneous rocks, 4 – amphibolite facies metasedimentary rocks, 5 – high-grade mafic rocks, 6 – metasomatic rocks, very low-grade metamafic rocks and ultrahigh temperature metamorphosed calc-silicate granulites; **B** – discrimination diagram according to Aubrecht et al. (2009), 1 – pyroxenes and peridotites, 2 – felsic and intermediate granulites, 3 – gneisses and amphibolites metamorphosed under pressure and temperature conditions transitional to granulite and amphibolite facies metamorphism, 4 – gneisses metamorphosed under amphibolite facies conditions; **C** – ternary diagram of the chemistry of detrital garnets in comparison with possible source areas (1 – Moravian Zone, 2 – Moldanubian Zone, 3 – Svratka Crystalline Complex, 4 – granites of the Brno Massif, 5 – migmatites of the Brno Massif, 6 – younger part of the Moravian-Silesian Paleozoic/Culmian), data from source rocks according to Otava et al. (2000), Čopjaková et al. (2002, 2005), Čopjaková (2007) and Buriánek et al. (2012); ALM – almandine, GRS – grossular, PRP – pyrope, SPS – spessartine

c-axis (2.0%). Cracks were recognised in almost all grains (97.2%). The high percentage of broken zircons indicates a predominantly high content of zircons with a high elongation value.

Colourless zircons form 43.5%, zircons with a pale colour 45.2%, brown 8.8%, and opaque zircons 2.5%. The proportion of zoned zircons was relatively low (9.5%), as were zircons with older cores (3.2%). Inclusions were recognised in 92.8% of the grains studied.

Elongation (the relationship between the length and width of crystals) was used as an indicator of possible host rocks, cooling rate and transport duration (Poldervaart, 1950; Hoppe, 1966; Zimmerle, 1979; Finger and Haunschmid, 1988). The average value of elongation of the zircons studied is 2.4 and the distribution of elongation is shown in Figure 13A. Zircons with elongation <2.5 are significantly more common (70.6%) than zircons with elongation >2.5 (29.4%). Zircons with an elonga-

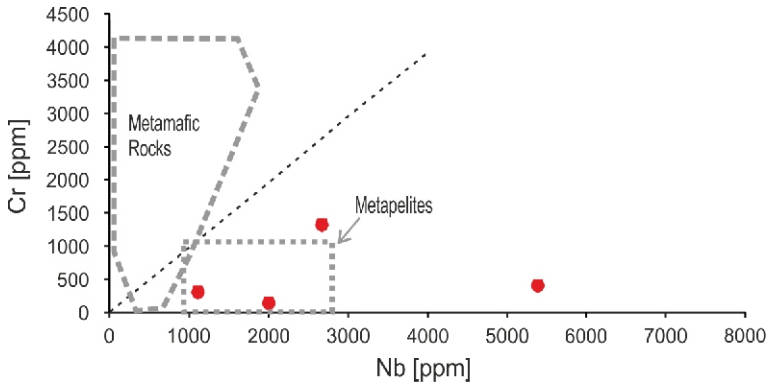

Fig. 12. Cr vs. Nb discrimination plot of the rutiles investigated

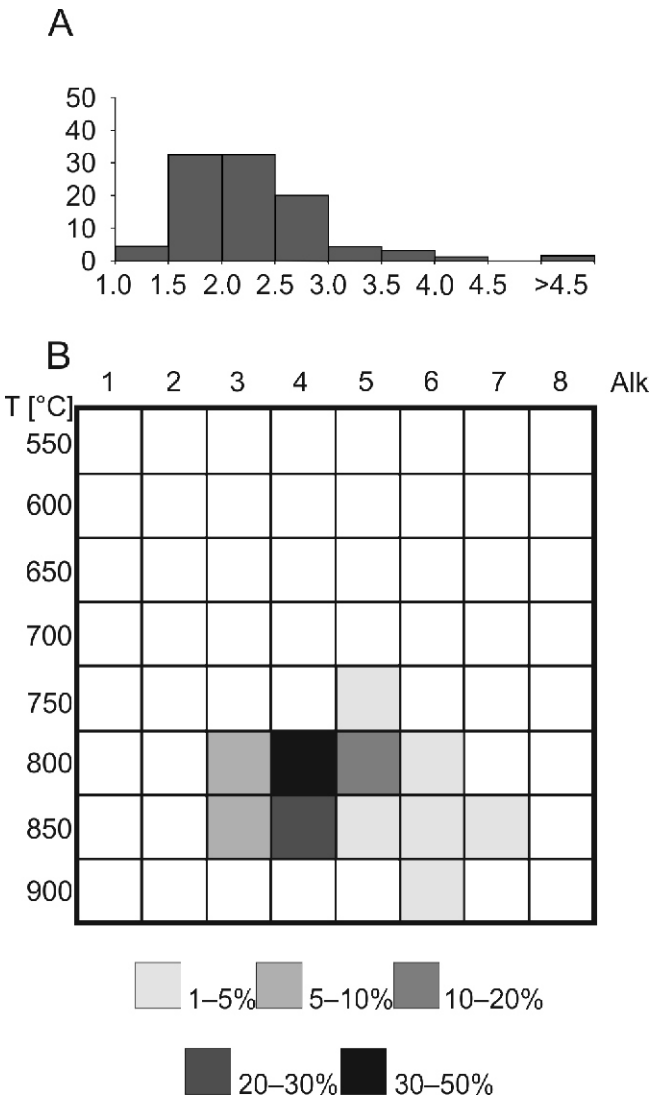

Fig. 13. Diagrams for the zircons studied

A – histogram of zircon elongation; **B** – typology of the zircons in the Pupin diagram (Pupin, 1980)

tion of >3 account for 9.2%. The maximum elongation was 5.7. However, the content of elongated zircons was probably initially higher, since many zircon grains are broken across the prism (i.e. parallel to the c-axis). Since the elongation of the broken long-prismatic zircons cannot be estimated, the population appears to be relatively less abundant (similarly Salata, 2014).

The evaluation of zircon typology according to Pupin (1980, 1985) is based on the external zircon faces (both pyramids and prisms). This method assumes that the parent magma (especially the aluminium and alkali content and the crystallisation temperature) show a correlation with the produced zircon subtype. A standard designation was proposed for 64 zircon subtypes (Pupin, 1980, 1985). In the case studied, a relatively narrow spectrum of subtypes has been recognised. The most frequent typological subtypes were S18 (41.3%), S23 (20.7%), and S19 (12.5%). Other subtypes, i.e., S17 (5.3%), S24 (2.9%), S22 (7.2%), S14 (1.9%), S25 (4.8%), S20 (1.0%), P5 (1%), S13 (0.5%), J5 (1%), were less common. The distribution and frequency of zircon subtypes in the typological diagram of Pupin (1980) are shown in Figure 13B.

INTERPRETATION OF PROVENANCE DATA

There is strong evidence that the gravel clasts of FA 3 were locally derived from the underlying granites of the Thaya Batholith. Weathering processes produced numerous gravel-sized clasts, grus, and also a large part of sand. In addition, the strong fracturing of the granite at the Waitzendorf fault certainly plays a major role in the formation of cobbles and boulders. In particular, the exposure with coarse cobble and boulder facies lies directly in the area of the Waitzendorf fault. The sands in the upper parts of the sedimentary sequences also carry a high proportion of lithic components from granites, indicating the input of a considerable amount of sedimentary material directly from the adjacent granites. A limited role of metamorphic rocks in the provenance was recognised in the pebble petrography of the FA 2 and FA 1 deposits.

On the other hand, the heavy mineral spectra generally indicate a major role of metamorphic rocks (both medium-grade/especially metapelites and high-grade/granulites, gneisses) in the source area. Significant differences in the heavy mineral assemblages of the nearby localities of the same formation may be connected with variations in the transport distances, role of local sources or the energy of the environment. Differences in heavy mineral spectra between Obermarkersdorf and Rosenau suggest an important role of local sources and rapid deposition with a short alongshore transport. A complex and complicated coastal palaeogeography with numerous small bays encourages such conditions. The higher role of zircon in heavy mineral spectra recognised at Rosenau is explained by a greater role of granites of the Thaya Batholith in provenance compared to Obermarkersdorf. A relatively low ZTR index indicates that the primary source is predominantly from crystalline rocks and that redeposition from older deposits played a minor role. The fluctuating heavy mineral assemblages/indices are inferred to be directly derived from alluvial/fluvial input that transported the weathered material to the nearshore environment.

For comparison, the ZTR index of the deposits from the Obermarkersdorf and Rosenau area are significantly lower than that of the deposits of the Burgschleinitz Formation from the exposures around Maigen in the Eggenburg Bay (Nehyba and Roetzel, 2021). However, the ATi and Gzi indices are higher at Obermarkersdorf and Rosenau. Here, variations in transport distances, sediment storage and recycling have also played an important role. Indices with more homogeneous/average values may be inferred to have been fed by sediments originally accumulated in nearshore environments or were recycled.

These results indicate that a higher amount of recycled material is present in the more basinward/distal areas (Eggenburg Bay, e.g., Maigen) and that primary and local sources played a greater role on the margins outside the Eggenburg Bay (e.g., Obermarkersdorf Basin). The primary material was probably intensely weathered (source area, alluvial storage, subaerial unconformities) (see Morton and Hallsworth, 1994). The provenance can be located in the nearby crystalline geological units such as the Moravian and Moldanubian Superunit and also the Thaya Batholith.

Significant variations in zircon shape-related attributes indicate several zircon sources. The strong dominance of S18, S22 and S19 subtypes in the zircon population, yielding a relatively well-defined concentration field (Fig. 13B), suggests that the euhedral zircons originated from a “single” source area and protolith type. The distribution of the main zircon crystal subtypes in the typological diagram is concentrated in the branches typical of magma with calc-alkaline affinity (Pupin, 1980; Sturm, 2010). The typological diagram shows an almost equal to

slightly higher occurrence of crystals with flat [101] pyramids versus steep ones [211] and a clear predominance of the prism form [100] over the prism form [110], which indicates a possible source from monzonite or granite (Caironi et al., 2000) and probably a hybrid character of the parent magma. Zircon shows a tendency to a crystal growth in a magmatic environment with a high content of calc-alkalic elements but decreased concentrations of Al (Sturm, 2010). The dominance of zircons with elongation below 2.5 indicates deep-lying, slowly cooled plutonic bodies (Corfu et al., 2013). However, the presence of highly elongated zircons also indicates that rapidly crystallised, porphyritic, sub-volcanic intrusions, high-level granites or volcanic rocks occurred in the source area and/or limited transport of grains (Zimmerle, 1979). The euhedral zircon data indicate that a part of the sediment was first cycle material, derived from crystalline/plutonic rocks. Highly energetic conditions of transport and deposition led to common breaking of the elongated zircons. These primary sources are traced to the nearby Thaya Batholith. However, rounded and well-rounded zircons must be differently sourced. There are several possible sources for them. The first is that some of the detritus had previously experienced sedimentary processes, i.e., it was subject to multiple recycling. Due to their mineral stability and hardness, zircon grains require extreme abrasion during transport to become rounded. Therefore, it is likely that well-rounded zircon grains (e.g., Mange and Maurer, 1992; Garzanti et al., 2015; Zoleikhaei et al., 2016) have undergone fluvial transport, littoral, or aeolian reworking during several sedimentary cycles. The large number of broken zircon grains and zircon grains with numerous collision marks on the surfaces indicate multiple reworking of the material. Therefore, a source from hypothetical older sedimentary rocks cannot be completely excluded. However, a second possible source of rounded zircon grains could be the metamorphic rocks of the nearby Moravian Superunit or even of the Moldanubian Superunit. Zircons from the Gföhl gneiss are described as well-rounded, colourless or pale coloured, and with an elongation between 1.78 and 2.27. Similarly, zircons from granulites are well-rounded and colourless (Niedermayr, 1967; Sturm, 2010).

A broader spectrum of the zircon source was corroborated by the chemical analysis of zircon. Although only three zircon grains were analysed, the Hf/Y ratio varies from 5.4 to 79.8. Alkaline rocks and alkaline metasomatites, mafic and intermediate rocks, and also felsitic rocks, are all suitable as possible source rocks (Belousova et al., 2002).

An accessory occurrence of apatite in the heavy mineral spectra seems to contradict the proposed important source from granites. However, a low content or absence of apatite is an almost typical feature of the Neogene deposits studied of the Alpine-Carpathian Foredeep. The explanation could be related to processes in the source area. Although apatite is stable during diagenesis, it is highly unstable during weathering and is therefore an important indicator of modification of sediment composition by weathering (Morton et al., 2012; Hurst and Morton, 2014).

The garnet data indicate the important role of the Moravian Superunit, especially the basal part of the Biteš gneiss and the Fugnitz calc-silicate rocks, as well as to the Lukov Unit, where calc-silicate rocks are moderately abundant. These sources are located ~10 km north-west from the exposures studied. Since the shoreline was clearly in close proximity to the localities, i.e., on the granitic bedrock of the Thaya Batholith, we have to look for some kind of sediment supply from the metamorphic provenance (as a primary source) into the basin. Lack of evidence of plant fragments, some metamorphic pebbles and low mineralogical maturity do not support fluvial/deltaic input. Therefore, a steep rocky shore and a delivery though small streams and/or terminal/alluvial fans are inferred.

DISCUSSION

In the Diem sand pit, cross-stratification, planar stratification and the considerable thickness of the nearshore succession in the lower part of the profile suggest a high-energy coastal setting (Clifton, 1981). Similarly, segregation of sand and gravel increases with wave energy (Hart and Plint, 1995). Microtidal conditions are inferred from the coarse grain size, the prevalence of wave-generated sedimentary structures and bedforms, the absence of tidal sedimentary structures, and also the low height of the gravel beach (Bluck, 2011). For these deposits of the Burgschleinitz Formation, a mixed fair-weather and storm origin is inferred.

By contrast, the gravel pits in the vicinity of Rosenau provide data on the uppermost, landward part of the Burgschleinitz Formation in the study area. There, the Burgschleinitz Formation overlies a bedrock surface that is interpreted in part as a rocky coast with high relief cliffs and ridges as well as pocket beaches and/or platforms cut by palaeo-waves.

The lithostratigraphic architecture of the Burgschleinitz Formation reflects the stepwise transgression in the Early Miocene onto the southeastern margin of the Bohemian Massif and the deposits studied might be interpreted as a partially preserved transgressive systems tract.

We can document two phases of transgression and successive overtopping of the basement with different coastal physiography. Two palaeogeographic sketches of the Obermarkersdorf Basin in the Early Miocene (late Eggenburgian) and the coastal evolution in the area under study are shown in Figure 14.

During the initial phase a barrier island complex developed with relatively fine-grained deposits (see Fig. 14A). This situation reflects flooding of the distant part of the Thaya Batholith and a relatively flat basement morphology (flooding trajectory). The lagoonal deposits of FA 4, which are sandwiched between foreshore deposits of FA 2, are interpreted as a part of a barrier island complex (Nummedal and Swift, 1987; Allen and Johnson, 2011). The preserved part of the complex represents its more landward (and deeper) facies. Waves mobilised the available sand and concentrated it along the coast into a barrier, which might have existed because the sediment supply was insufficient to fill the basin landward of the barrier (Boyd et al., 1992). The relict preservation of FA 4 reflects transgression from SE to N–NW and may have been influenced by the seafloor configuration prior to the transgression. Roughly tabular geometries are expected for the deposits of the initial phase.

The dominant portion of this transgressive stage is represented by the upper shoreface deposits of FA 1. The predominance of trough and planar cross-stratification in FA 1 implies that dunes were the dominant bedform on the shoreface. It is unlikely that these are tidal bedforms due to the absence of sedimentary structures indicative for tidal activity. The complex internal arrangement of the cross-stratified bed, cut by several second-order surfaces and containing subordinate interbeds of facies Sb and Sr, is interpreted as evidence of fluctuations of current velocity, probably during storm and fair-weather periods (DeCelles, 1987). Such a situation may be interpreted as evidence of particularly high-energy currents that allowed erosion of most of the deposits related to the recovery period of the previous storm cycle. Evidence of thick-bedded cross-stratification is reminiscent of a barred shoreface (Wignall et al., 1996). The absence of suspended fine-grained deposits with little evidence

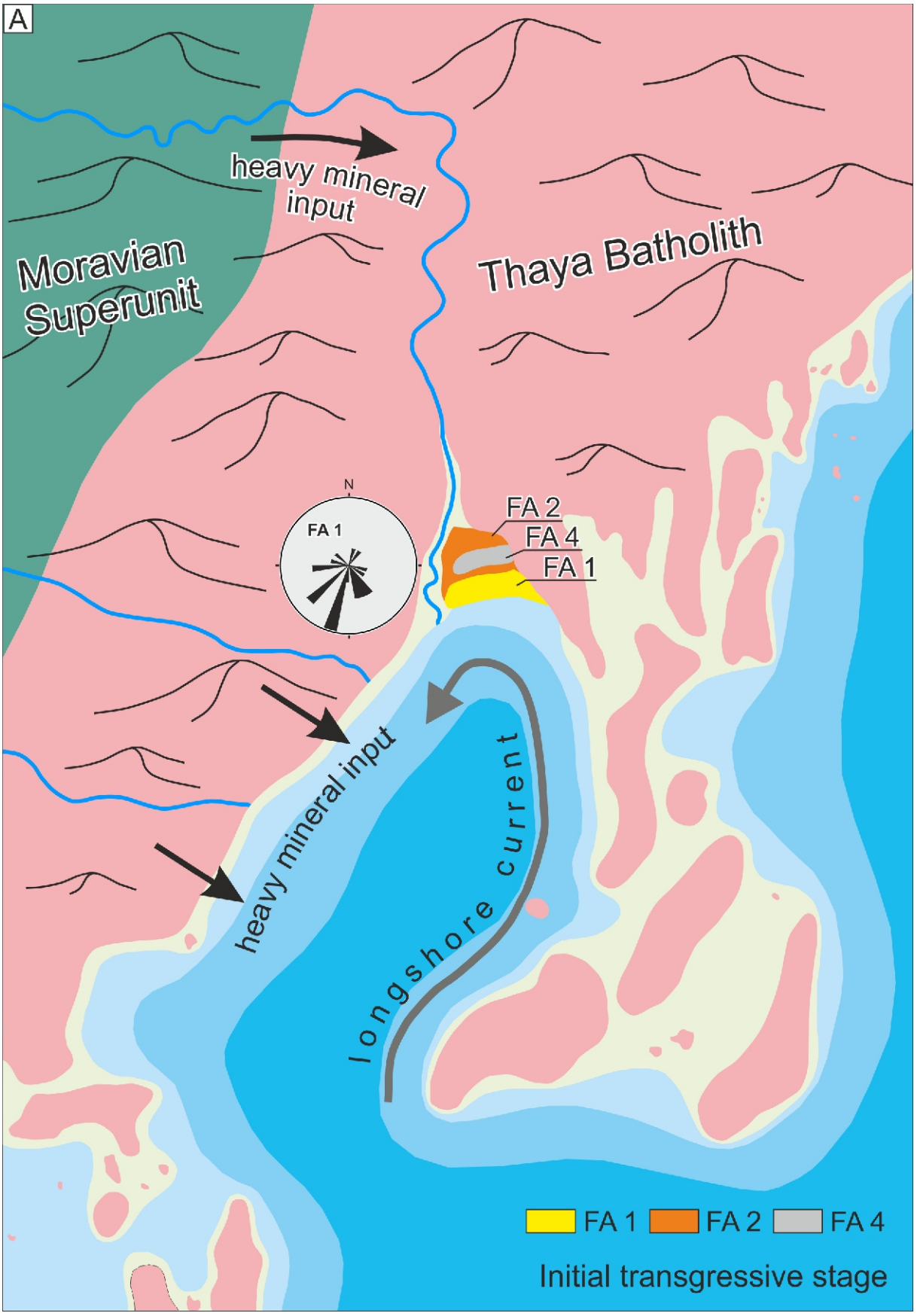

Fig. 14. Schematic maps of the Early Miocene (Eggenburgian) palaeogeography, sedimentation, sediment sources and successive overtopping in the Obermarkersdorf Basin

A – the coastal system during the initial transgressive stage of flooding of the distal parts of the Thaya Batholith with flatter basement morphology and formation of a barred shoreline with transport directions (rose diagram – FA 1/ Diem sand pit); **B** – the successive second stage of transgression with flooding of more proximal parts of the Thaya Batholith – rocky shoreline with transport directions (rose diagram – FA 3 / Rosenau gravel pits)

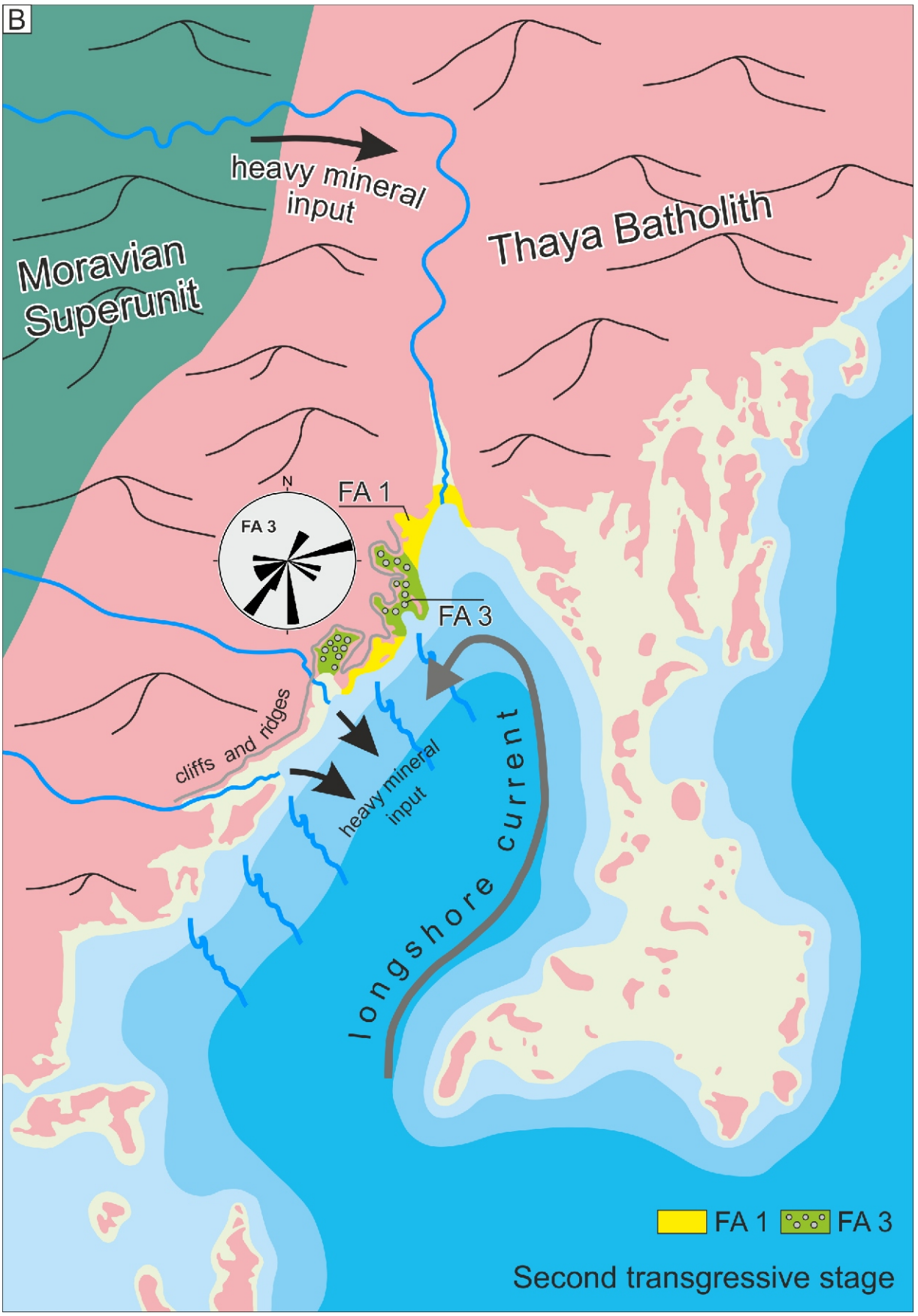
B
heavy mineral input
Moravian Superunit
Thaya Batholith
N
FA 1
FA 3
FA 3
cliffs and ridges
heavy mineral input
longshore current
FA 1
FA 3
Second transgressive stage

of bioturbation suggests that dunes migrated almost continuously, an attribute of fair-weather conditions (Wignall et al., 1996), while the palaeocurrent pattern may reflect the occurrence of several distinct currents. During major storms, erosion may have affected not only the beachface but also the shoreface, particularly the upper shoreface (Elliott, 1986). The erosion surfaces at the bases of gravel layers may represent the records of the peaks of such events. Nearshore bars develop best along shorelines intermediate between the low-energy reflective and the high-energy dissipative beach zones (Clifton, 2006). Conditions favouring their development include moderate prevailing breaker heights (1 to 2.5 m), tidal range <1.5 m, medium grain size, and meagre to moderate sediment supply. The basal unconformity of the Burgschleinitz Formation represents both a sequence boundary (a basal unconformity with evidence for subaerial weathering) and a transgressive erosion surface.

The successive phase of transgression led to the flooding of the more proximal parts of the Thaya Batholith with a much steeper relief (see Fig. 14B). A significant part of the barrier island complex was eroded. The superposition of the coarse-grained foreshore sub-association FA 2b over FA 4 in the Diem sand pit points to wave-cut erosion (a wave ravinement surface) on the retreating shoreface during transgression. The shoreface sands of FA 1 erosively overlain by foreshore deposits of FA 2 (mostly with pebble lag of Gm facies; Fig. 4), or locally replaced by beachface gravels of FA 3 (Fig. 5) are further evidence of shoreface retreat correlated with a marine flooding surface/ravinement surface in general. The gravelly deposits of FA 3 might have been topographically "trapped" and "backed up" against pre-existing relief (headlands, palaeo-sea cliffs, palaeo-wave-cut platforms, etc.; Johnson, 1988; Evans and Holm-Denoma, 2018). These deposits tend to be relatively thin, laterally discontinuous or restricted.

Poorly sorted, coarse-grained but silty and highly bioturbated deposits with a high content of lithic components from granites recorded in the Diem sand pit in the uppermost part of the profile (currently not available for study) reflect the continuing deepening of the depositional environment associated with a successive phase of transgression. These deposits may be interpreted as lower shoreface deposits.

Deposits of both stages of the transgressive phase reveal internal evidence of a shallowing-upwards (coarsening-upwards as well) and progradational settings. Such signals are the superposition of backshore deposits of FA 4 over the fine-grained foreshore sub-association FA 2a and superposition of FA 2 over FA 1 in the higher portion of the succession (Fig. 4). Similarly, a vertical succession of gravel zones in FA 3 and a crude upwards-coarsening trend (evident by the presence of boulders) reflect progradation, as the coarsest clasts are mostly found in the uppermost/landward part of the beachface (Massari and Parea, 1988; Hart and Plint, 1995; Bluck, 2011). These progradational packages correspond to parasequences. A stacked set of progradational parasequences separated by erosional surfaces formed during the regional transgression and general shoreface retreat is supposed for the succession studied.

The gravelly beach deposits of FA 3 are interpreted as evidence of a rocky shoreline due to their direct position on the crystalline basement and clast lithologies strictly limited to the underlying unit (which served as the sediment source). The beachface tabular cobble and boulder gravels were probably sourced from rock talus. In addition, the strong fracturing of the granite on the Waitzendorf fault encouraged the formation of cobbles and boulders. Rocky shoreline deposits provide information about sea-level position, coastal morphology, sediment source-to-sink relationships and other parameters at a specific time in the geological history of the region, but have very low preservation potential in the geological record (Johnson, 2006). Geological mapping also allows the estimation of a shoreline trend that forms a small bay like pocket beach in the study area. We infer a complex coastal morphology with a palaeo-relief of about several metres.

Textural trends in the gravels of FA 2 and of FA 3 reveal clast size fining away from the sediment source area. This is accompanied by a wider provenance of the granules and small pebbles. An additional source from metamorphic rocks is clearly reflected in the heavy mineral spectra. For the source from the granites of the Thaya Batholith, erosion of the beachface sediments and their offshore redeposition was responsible. When comparing the gravels of FA 2 and FA 3, a mixing of different predominantly granulometric and to a lesser extent morphometric clast populations was observed. Additionally, longitudinal transport, connected with longshore drift, is inferred to be responsible for the source from metamorphic rocks. The role of longitudinal transport is evident when we compare the petrography of the Obermarkersdorf and Maigen localities.

Palaeocurrent data (n = 39) from clast long-axis orientations, imbrication and cross-stratification indicate SW, S to NE transport, roughly onshore-offshore to a coastline. The shoreline orientation and regional palaeogeography are based on detailed geological mapping. However, typical bimodal onshore and offshore directions associated with shoaling waves and storm currents are not developed. The pebbles dip mostly towards S-SW, i.e., generally offshore. The pebble layers suggest winnowing of finer-grained material by combined oscillatory and unidirectional currents (with a dominant role of offshore currents), and seawards-inclined sheets of gravel with low relief. The onshore component is less well developed. Palaeocurrents of the cross-stratified beds indicate prevailing flow directions towards the S or SW, which are interpreted as a dominant unidirectional component perpendicular to the palaeo-shoreline and offshore-directed superimposed on the oscillatory flow. Cross-stratification dips offshore at angles ranging from 10° to 30°. The rest of the palaeocurrents are shore-oblique or onshore. The longshore currents are probably responsible for the shore-oblique directions. The onshore cross-stratification is uncommon, indicating that dunes produced by fair-weather waves are rarely preserved (Chiocci and Clifton, 1991). According to Clifton (2006) bedforms which faced seaward and produced seawards-dipping cross-stratification are located adjacent to the beach foreshore.

CONCLUSIONS

The combination of facies and provenance analysis with detailed geological mapping allowed identification of the depositional environment, reconstruction of the palaeo-coastline position and morphology, sediment source-to-sink relationships, and other parameters of the Lower Miocene (Lower Burdigalian/Eggenburgian) deposits of the Burgschleinitz Formation in part of the Alpine-Carpathian Foredeep on the margin of Thaya Batholith.

The Burgschleinitz Formation overlies a basement surface with basal unconformity (transgressive erosional surface) that shows evidence of subaerial weathering. The deposits of the Burgschleinitz Formation recognised can be divided into four facies associations/depositional environments, i) upper-shoreface, ii) foreshore, iii) gravelly beach and iv) backshore – lagoon, which indicate high-energy coastal settings, microtidal conditions and a mixed fair-weather and storm

origin. The lithostratigraphic architecture of the Burgschleinitz Formation reflects a stepwise transgression onto the southeastern margin of the Bohemian Massif. The deposits are interpreted as a transgressive systems tract.

Two stages of transgression and successive overtopping of the basement with different coastal physiography were documented. During the initial stage of transgression (from SE and E towards the N–NW), a barrier island complex developed with relatively fine-grained deposition, reflecting flooding of the distant part of the Thaya Batholith, with a relatively flat basement morphology. A subsequent continuation of transgression led to the flooding of the more proximal parts of the Thaya Batholith with a steeper relief, and formation of a rocky shoreline with deposition of gravelly deposits along palaeo-sea cliffs or wave-cut platforms. A complex coastal morphology is inferred with a palaeo-relief of ~50 m and with numerous crystalline ridges.

There is strong evidence that especially the gravel clasts of the deposits of the Burgschleinitz Formation investigated were derived directly from the underlying granites of the Thaya Batholith, with other rocks playing only a subordinate role in the source area. On the other hand, the heavy mineral studies indicate that metamorphic rocks (both medium-grade/especially metapelites and high-grade/granulites, gneisses) played an important role in provenance, mainly from the Moravian Superunit and particularly from calc-silicate rocks. These sources are generally located ~10 km west of the area studied (i.e., backshore behind the inferred coastline). This source material is supposed to have been delivered primarily by small creeks and alluvial fans into the nearshore. Significant differences in the heavy mineral assemblage of nearby localities of the same formation suggest a priority of local sources and rapid deposition with subordinate influence of longshore transport, which might be related to a complex and complicated coast palaeogeography.

These Lower Miocene deposits of the Burgschleinitz Formation provide evidence of the evolution of a rocky shoreline, which generally have a very low preservation potential in the geological record.

Acknowledgements. Fieldwork and laboratory costs from the Geological Survey of Austria and by the institutional support of the Faculty of Science of Masaryk University Brno 1363 “Formation and evolution of the depositional basins of the Bohemian Massif and Western Carpathians preserved in their sedimentary record” are gratefully acknowledged.

We would like to thank Mrs. A. Diem very much for permission to do fieldwork in her sand pit. We thank O. Mandic and M. Harzhauser for their support in mollusc determination and biofacies interpretation. Andreas Thinschmidt and Ingeborg Wimmer-Frey have carried out parts of the heavy mineral and light mineral investigations many years ago, for which we would also like to thank them. M. Harzhauser and an anonymous reviewer are thanked for valuable advice and useful comments on the manuscript.

REFERENCES

Allen, J.L., Johnson, C.L., 2011. Architecture and formation of transgressive-regressive cycles in marginal marine strata of the John Henry Member, Straight Cliffs Formation, Upper Cretaceous of Southern Utah, USA. Sedimentology, **58**: 1486–1513.

Aubrecht, R., Méres, Š., Sýkora, M., Mikus, T., 2009. Provenance of the detrital garnets and spinels from the Albian sediments of the Czorsztyn Unit (Pieniny Klippen Belt, Western Carpathians, Slovakia). Geologica Carpathica, **60**: 463–483.

Belousova, E.A., Griffin, W.L., O’Reilly, S.Y., Fisher, N.I., 2002. Igneous zircon: trace element composition as an indicator of source rock type. Contributions to Mineralogy and Petrology, **143**: 602–622.

Bluck, B.J., 1967. Sedimentation of beach gravels: examples from South Wales. Journal of Sedimentary Petrology, **37**: 128–156.

Bluck, B.J., 1999. Clast assembling, bed-forms and structure in gravel beaches. Earth and Environmental Science Transactions of the Royal Society of Edinburg, **89**: 291–323.

Bluck, B.J., 2011. Structure of gravel beaches and their relationship to tidal range. Sedimentology, **58**: 994–1006.

Boyd, R., Dalrymple, R.W., Zaitlin, B.A., 1992. Classification of clastic coastal depositional environments. Sedimentary Geology, **80**: 139–150.

Buriánek, D., Tomanová Petrová, P., Otava, J., 2012. Where do the Miocene sediments of the Brno region come from? (in Czech with English summary). Acta Musei Moraviae, Sciences Geology, **97**: 153–156.

Caironi, V., Colombo, A., Tunesi, A., Gritti, C., 2000. Chemical variations of zircon compared with morphological evolution during magmatic crystallization: an example from the Valle del Cervo Pluton (Western Alps). European Journal of Mineralogy, **12**: 779–794.

Cattaneo, A., Steel, R.J., 2003. Transgressive deposits: a review of their variability. Earth-Science Reviews, **62**: 187–228.

Chiocci, F.C., Clifton H.E., 1991. Gravel-filled gutter casts in nearshore facies-indicators of ancient shoreline trend. SEPM Special Publication, **46**: 67–76.

Clifton, H.E., 1981. Progradational sequences in Miocene shoreline deposits, southeastern Caliente Range, California. Journal of Sedimentary Research, **51**: 165–184.

Clifton, H.E., 2006. A reexamination of facies models for clastic shorelines. SEPM Special Publication, **84**: 293–338.

Collins, D.S., Johnson, H.D., Allison, P.A., Guilpain, P., Damit, A.R., 2017. Coupled “storm-flood” depositional model: Application to the Miocene-Modern Baram Delta Province, north-west Borneo. Sedimentology, **64**: 1203–1235.

Collinson, J.D., Mountney, N. P., Thompson, D.B., 2006. Sedimentary Structures. 3rd ed., Terra Publishing, Harpenden.

Čopjaková, R., 2007. The reflection of provenance changes in the psefitic and psamitic sedimentary fraction of the Myslejovice Formation (heavy mineral analysis) (in Czech). Ph.D. thesis, Masaryk University, Brno.

Čopjaková, R., Sulovský, P., Otava, J., 2002. Comparison of the chemistry of detritic pyrope-almandine garnets of the Luleč Conglomerates with the chemistry of granulite garnets from the Czech Massif (in Czech). Geologické výzkumy na Moravě a ve Slezku v roce 2001, **9**: 44–47.

Corfu, F., Hanchar, J.M., Kinny, P., 2013. Atlas of zircon textures. Reviews in Mineralogy and Geochemistry, **53**: 468–500.

DeCelles, P.G., 1987. Variable preservation of Middle Tertiary, coarse-grained, nearshore to outer-shelf storm deposits in southern California. Journal of Sedimentary Petrology, **57**: 250–264.

Droser, M.L., Bottjer, D.J., 1986. A semiquantitative field classification of ichnofabric. Journal of Sedimentary Research, **56**: 558–559.

Dumas, S., Arnott, R.W.C., 2006. Origin of hummocky and swaley cross-stratification – the controlling influence of unidirectional current strength and aggradation rate. Geology, **34**: 1073–1076.

Elliott, T., 1986. Siliciclastic shorelines. In: Sedimentary Environments and Facies (ed. H. G. Reading): 155–188. Blackwell Scientific Publications.

Evans, J.E., Holm-Denoma, C.S., 2018. Processes and facies relationships in a Lower(?) Devonian rocky shoreline depositional environment, East Lime Creek Conglomerate, south-western Colorado, USA. The Depositional Record, **4**: 133–156.

Finger, F., Haunschmid, B., 1988. Die mikroskopischen Untersuchungen der akzessorischen Zirkone als Methode zur Klärung der Intrusionsfolge in Granitgebieten – eine Studie im nordöstlichen oberösterreichischen Moldanubikum. Jahrbuch der Geologischen Bundesanstalt, **131**: 255–266.

Folk, R.L., 1968. Petrology of Sedimentary Rocks. Austin, Texas, Hemphill's Bookstore.

Folk, R.L., Ward, W., 1957. Brazos River bar: a study in the significance of grain-size parameters. Journal of Sedimentary Research, **27**: 3–26.

Force, E.R., 1980. The provenance of rutile. Journal of Sedimentary Research, **50**: 485–488.

Friedman, G.M., 1962. On sorting, sorting coefficients and the lognormality of the grain-size distribution of sandstones. The Journal of Geology, **70**: 737–753.

Garzanti, E., Resentini, A., Ando, S., Vezzoli, G., Pereira, A., Vermeesch, P., 2015. Physical controls on sand composition and relative durability of detrital minerals during ultra-long distance littoral and aeolian transport (Namibia and southern Angola). Sedimentology, **62**: 971–996.

Girty, G.H., Marsh, J., Meltzner, A., McConnell, J.R., Nygren, D., Nygren, J., Prince, G.M., Randall, K., Johnson, D., Heitman, B., Nielsen, J., 2003. Assessing changes in elemental mass as a result of chemical weathering of granodiorite in a Mediterranean (hot summer) climate. Journal of Sedimentary Research, **73**: 434–443.

Hart, B.S., Plint, A.G., 1989. Gravelly shoreface deposits: a comparison of modern and ancient facies sequences. Sedimentology, **36**: 551–557.

Hart, B.S., Plint, A.G., 1995. Gravelly shoreface and beachface deposits. IAS Special Publication, **22**: 75–99.

Hartley, A.J., Jolley E.J., 1999. Unusual coarse, clastic, wave-dominated shoreface deposits, Pliocene to Middle Pleistocene, northern Chile: implications for coastal facies analysis. Journal of Sedimentary Research, **69**: 105–114.

Hoppe, G., 1966. Zirkone aus Granuliten. Berichte der Deutschen Gesellschaft für Geologische Wissenschaften – Reihe B, **11**: 47–81.

Hubert, J.F., 1962. A zircon-tourmaline-rutile maturity index and the interdependence of the composition of heavy mineral assemblages with the gross composition and texture of sandstones. Journal of Sedimentary Research, **32**: 440–450.

Hurst, A., Morton, A., 2014. Provenance models: the role of sandstone mineral–chemical stratigraphy. Geological Society Special Publications, **386**: 7–26.

Johnson, M.E., 1988. Why are ancient rocky shorelines so uncommon? Journal of Geology, **96**: 469–480.

Johnson, M.E., 2006. Uniformitarianism as a guide to rocky-shore ecosystems in the geologic record. Canadian Journal of Earth Sciences, **43**: 1119–1147.

Kern, H.P., Lavina, E.L.C., Palm, P.S.G., Leanza, H.A., 2019. Stratigraphic evolution of the nearshore to fluvial plain of the Upper Cuyo Group, Neuquén, Argentina. Sedimentology, **66**: 2686–2720.

Kühn, O., 1955. Die Bryozoen der Retzer Sande. Sitzungsberichte der Akademie der Wissenschaften, mathematisch-naturwissenschaftliche Klasse, Abteilung I, **164**: 231–248.

Lamb, M.P., Myrow, P.M., Lukens, C., Houck, K., Strauss, J., 2008. Deposits from wave-influenced turbidity currents: Pennsylvanian Minturn Formation, Colorado, U.S.A. Journal of Sedimentary Research, **78**: 480–498.

Leckie, D., 1987. Wave-formed, coarse-grained ripples and their relationship to hummocky cross-stratification. Journal of Sedimentary Petrology, **58**: 607–622.

Lihou, J.C., Mange-Rajetzky, M.A., 1996. Provenance of the Sardona Flysch, eastern Swiss Alps: example of high-resolution heavy mineral analysis applied to an ultrastable assemblage. Sedimentary Geology, **105**: 141–157.

Longhitano, S., Chiarella, D., Di Stefano, A., Messina, C., Sabato, L., Tropeano, M., 2012. Tidal signatures in Neogene to quaternary mixed deposits of southern Italy straits and bays. Sedimentary Geology, **270**: 74–96.

Mader, D., 1980. Weitergewachsene Zirkone im Bundsandstein der Westeifel. Der Aufschluss, **31**: 163–170.

Maejima, W., 1982. Texture and stratification of gravelly beach sediments, Enju Beach, Kii Peninsula, Japan. Journal of Geoscience, Osaka City University, **25**: 35–51.

Mandic, O., Harzhauser, M., 1999. Pectiniden (Bivalvia) als Faziesindikatoren im Eggenburgium der Retz-Formation. In: Arbeitstagung der Geologischen Bundesanstalt 1999, Retz-Hollabrunn, 3–7 Mai 1999, Wien (ed. R. Roetzel): 231–232.

Mandic, O., Steininger, F.F., 2003. Computer-based mollusc stratigraphy – a case study from the Eggenburgian (Lower Miocene) type region (NE Austria). Palaeogeography, Palaeoclimatology, Palaeoecology, **197**: 263–291.

Mange, M.A., Maurer, H.F.W., 1992. Heavy Minerals in Colour. Chapman and Hall, London.

Mange, M.A., Morton A.C., 2007. Geochemistry of heavy minerals. Developments in Sedimentology, **58**: 345–391.

Massari, F., Parea, G.C., 1988. Progradational gravel beach sequences in a moderate- to high-energy, microtidal marine environment. Sedimentology, **35**: 881–913.

Meinhold, G., Anders, B., Kostopoulos, D., Reischmann, T., 2008. Rutile chemistry and thermometry as provenance indicator: an example from Chios Island, Greece. Sedimentary Geology, **203**: 98–111.

Morton, A.C., Hallsworth, C.R., 1994. Identifying provenance-specific features of detrital heavy mineral assemblages in sandstones. Sedimentary Geology, **90**: 241–256.

Morton, A.C., Hallsworth, C.R., 1999. Processes controlling the composition of heavy mineral assemblages in sandstones. Sedimentary Geology, **124**: 3–29.

Morton, A.C., Mundy, D.J.C., Bingham, G., 2012. High-frequency fluctuations in heavy mineral assemblages from Upper Jurassic sandstones of the Piper Formation, UK North Sea: relationships with sea level change and floodplain residence. GSA Special Paper, **487**: 163–176.

Myrow, P.M., 1992. Pot and gutter casts from Chapel Island Formation, southeast Newfoundland. Journal of Sedimentary Research, **62**: 992–1007.

Myrow, P.M., Southard, J.B., 1996. Tempestite deposition. Journal of Sedimentary Research, **66**: 875–887.

Nalin, R., Massari, F., 2009. Facies and stratigraphic anatomy of a temperate carbonate sequence (Capo Colonna terrace, Late Pleistocene, southern Italy). Journal of Sedimentary Research, **79**: 210–225.

Nalin, R., Ghinassi, M., Foresi, L.M., Dallanave, E., 2016. Carbonate deposition in restricted basins: a Pliocene case study from the Central Mediterranean (Northwestern Apennines), Italy. Journal of Sedimentary Research, **86**: 236–267.

Nebelsick, J., 1989. Temperate water carbonate facies of the Early Miocene Paratethys (Zogelsdorf Formation, Lower Austria). Facies, **21**: 11–40.

Nehyba, S., Roetzel, R., 2021. Coastal sandy spit deposits (Lower Burdigalian/Eggenburgian) in the Alpine-Carpathian Foredeep of Lower Austria. Geological Quarterly, **65**: 50.

Nemec, W., Steel, R.J., 1984. Alluvial and coastal conglomerates: Their significant features and some comments on gravelly mass flow deposits. Canadian Society of Petroleum Geologists Memoir, **10**: 1–31.

Niedermayr, G., 1967. Die akzessorischen Gemengteile von Gföhler Gneis, Granitgneis und Granulit im niederösterreichischen Waldviertel. Annalen des Naturhistorischen Museums Wien, **70**: 19–27.

Nummedal, D., Swift, D.J.P., 1987. Transgressive stratigraphy at sequence-bounding unconformities: some principles derived from Holocene and Cretaceous example. SEPM Special Publication, **41**: 241–260.

Okada, H., 1971. Classification of sandstone: analysis and proposal. The Journal of Geology, **79**: 509–525.

Otava, J., Sulovský, P., Čopjaková, R., 2000. Provenance changes of the Drahany Culm greywackes: statistical evaluation (in Czech). Geologické výzkumy na Moravě a ve Slezku v r. 1999: 94–98.

Pettijohn, F.J., Potter, P.E., Siever, R., 1987. Sand and Sandstone. 2nd edition, Springer-Verlag, New York.

Piller, W.E., Harzhauser, M., Mandic, O., 2007. Miocene Central Paratethys stratigraphy – current status and further directions. Stratigraphy, **4**: 151–168.

Poldervaart, A., 1950. Statistical studies of zircon as a criterion in granitization. Nature, **165**: 574–575.

Postma, G., Nemec, W., 1990. Regressive and transgressive sequences in a raised Holocene gravelly beach, southwestern Crete. Sedimentology, **37**: 907–920.

Powers, M.C., 1953. A new roundness scale for sedimentary particles. Journal of Sedimentary Petrology, **23**: 117–119.

Pupin, J.P., 1980. Zircon and granite petrology. Contributions to Mineralogy and Petrology, **73**: 207–220.

Pupin, J.P., 1985. Magmatic zoning of hercynian granitoids in France based on zircon typology. Schweizerische mineralogische und petrographische Mitteilungen, **65**: 29–56.

Reineck, H.-E., Singh, I.B., 1980. Depositional Sedimentary Environments. 2nd ed., Springer, Berlin-Heidelberg-New York.

Roetzel, R., 1996. Bericht 1994/1995 über geologische Aufnahmen im Tertiär und Quartär mit Bemerkungen zur Tektonik am Diendorfer Störungssystem auf Blatt 22 Hollabrunn. Jahrbuch der Geologischen Bundesanstalt, **139**: 286–295.

Roetzel, R., Heinrich, M., 1999. A1 Obermarkersdorf – Sandgrube Diem. In: Arbeitstagung der Geologischen Bundesanstalt 1999, Retz-Hollabrunn, 3–7 Mai 1999, Wien (ed. R. Roetzel): 261–263.

Roetzel, R., Kurzweil, H., 1986. Die Schwerminerale in niederösterreichischen Quarzsanden und ihre wirtschaftliche Bedeutung. Archiv für Lagerstättenforschung der Geologischen Bundesanstalt, **7**: 199–216.

Roetzel, R. [Bearbeitung]; **Batík, P., Cicha, I., Havlíček, P., Holásek, O., Novák, Z., Pálenský, P., Roetzel, R., Rudolský, J., Růžička, M., Stráník, Z., Švábenická, L., Vůjta, M.** [Geol. Aufnahme], **Hofmann, Th**. [Naturdenkmalbuch], **Hellerschmidt-Alber, J.** [Störungen - Satellitenbild- und Luftbildauswertung], **1998**. Geologische Karte der Republik Österreich 1:50.000 22 Hollabrunn. Wien (Geologische Bundesanstalt).

Roetzel, R., Fuchs, G. (österreichischer Anteil)**, Batik, P., Ctyroky, P.** (tschechischer Anteil) [Bearbeitung]**; Batik, P., Ctyroka, J., Ctyroky, P., Dudek, A., Fuchs, G., Havlicek, P., Matejovska, O., Roetzel, R.** [geol. Aufnahme]**, Hofmann, Th.** [Naturschutzbuch]**, 1999a**. Geologische Karte der Republik Österreich 1:50.000 9 Retz. Wien (Geologische Bundesanstalt).

Roetzel, R., Mandic, O., Steininger, F.F., 1999b. Lithostratigraphie und Chronostratigraphie der tertiären Sedimente im westlichen Weinviertel und angrenzenden Waldviertel. In: Arbeitstagung der Geologischen Bundesanstalt 1999, Retz-Hollabrunn, 3–7 Mai 1999 (ed. R. Roetzel): 38–54, Wien.

Roetzel, R., mit Beiträgen von **Fuchs, G., Havlíček, P., Übl, Ch., Wrbka, Th., 2005**. Geologie im Fluss. Erläuterungen zur Geologischen Karte der Nationalparks Thayatal und Podyjí. Wien (Geologische Bundesanstalt).

Roštínský, P., Roetzel, R., 2005. Exhumed Cenozoic landforms on the SE flank of the Bohemian Massif in the Czech Republic and Austria. Zeitschrift für Geomorphologie: Neue Folge, **49**: 23–45.

Salata, D., 2014. Advantages and limitations of interpretations of external morphology of detrital zircon: a case study of the Ropianka and Menilite formations (Skole nappe, Polish Flysch Carpathians). Annales Societatis Geologorum Poloniae, **84**: 153–165.

Schubert, G., Safoschnik, T., Supper, R., Bernhard, M., Felfer, W., Roetzel, R., 1999. B1 Das Becken von Obermarkersdorf. In: Arbeitstagung der Geologischen Bundesanstalt 1999, Retz-Hollabrunn, 3–7 Mai 1999 (ed. R. Roetzel): 279–286, Wien.

Sturm, R., 2010. Morphology and growth trends of accessory zircons from various granitoids of the South-western Bohemian Massif (Moldanubicum, Austria). Chemie der Erde, **70**: 185–196.

Tolosana-Delgado, R., von Eynatten, H., Krippner, A., Meinhold, G., 2018. A multivariate discrimination scheme of detrital garnet chemistry for use in sediment provenance analysis. Sedimentary Geology, **375**: 14–26.

Triebold, S., von Eynatten, H., Luvizotto, G.L., Zack, T., 2007. Deducing source rock lithology from detrital rutile geochemistry: An example from the Erzgebirge, Germany. Chemical Geology, **244**: 421–436.

Triebold, S., von Eynatten, H., Zack, T., 2012. A recipe for the use of rutile in sedimentary provenance analysis. Sedimentary Geology, **282**: 268–275.

Vávra, N., 1979. Die Bryozoenfauna des österreichischen Tertiärs. Neues Jahrbuch für Geologie und Paläontologie Abhandlungen, **157**: 366–392.

Vávra, N., 1981. Bryozoa from the Eggenburgian (Lower Miocene, Central Paratethys) of Austria. In: Recent and Fossil Bryozoa, (eds. G.P. Larwood and C. Nielsen): 273–280. Fredensborg.

Walker, R.G., James, N.P., 1992. Facies Models: Response to Sea Level Changes. Geological Association of Canada, St. John's.

Watkins, R., 1992. Sedimentology and paleoecology of Pliocene shallow marine conglomerates, Salton trough region, California. Palaeogeography, Palaeoclimatology, Palaeoecology, **95**: 319–333.

Whitaker, J.H.McD., 1973. "Gutter casts", a new name for scour-and-fill structures: with examples from the LLandoverian of Ringerike and Malmöya, southern Norway. Norsk Geologisk Tidsskrift, **53**: 403–417.

Wignall, P.B., Sutcliffe, O.E., Clemson, J., Young, E., 1996. Unusual shoreface sedimentology in the Upper Jurassic of the Boulonnais, northern France. Journal of Sedimentary Research, **60**: 577–586.

Winter, J., 1981. Exakte tephrostratigraphische Korrelation mit morphologisch differenzierten Zirkonpopulationen (Grenzbereich Unter-/Mitteldevon, Eifel-Ardennen). Neues Jahrbuch für Geologie und Paläontologie Abhandlungen, **162**: 97–136.

Yoshida, S., Steel, R.J., Dalrymple, R.W., 2007. Changes in depositional processes - an ingredient in a new generation of sequence-stratigraphic models. Journal of Sedimentary Research, **77**: 447–460.

Zack, T., von Eynatten, H., Kronz, A., 2004a. Rutile geochemistry and its potential use in quantitative provenance studies. Sedimentary Geology, **171**: 37–58.

Zack, T., Moraes, R., Kronz, A., 2004b. Temperature dependence of Zr in rutile: empirical calibration of a rutile thermometer. Contributions to Mineralogy and Petrology, **148**: 471–488.

Zecchin, M., 2007. The architectural variability of small-scale cycles in shelf and ramp clastic systems: the controlling factors. Earth-Science Reviews, **84**: 21–55.

Zimmerle, W., 1979. Accessory Zircon from Rhyolite, Yellowstone National Park (Wyoming, U.S.A.). Zeitschrift der deutschen Geologischen Gesellschaft, **130**: 361–369.

Zingg, Th., 1935. Beiträge zur Schotteranalyse. Schweizerische mineralogische und petrographische Mitteilungen, **15**: 39–140.

Zoleikhaei, Y., Frei, D., Morton, A., Zamanzadeh, M.S., 2016. Roundness of heavy minerals (zircon and apatite) as a provenance tool for unravelling recycling: a case study from the Sefidrud and Sarbaz rivers in N and SE Iran. Sedimentary Geology, **342**: 106–117.